Identifying the anti-inflammatory potential of α7 nicotinic receptor silent agonists in human blood immune cells

by

Eduardo Carlos Soto

A thesis submitted in partial fulfillment
of the requirements for the degree of
Master of Science (MSc) in Biology

The Faculty of Graduate Studies
Laurentian University
Sudbury, Ontario, Canada

THESIS DEFENCE COMMITTEE/COMITÉ DE SOUTENANCE DE THÈSE
Laurentian Université/Université Laurentienne
Faculty of Graduate Studies/Faculté des études supérieures

Title of Thesis Titre de la thèse	Identifying the anti-inflammatory potential of α7 nicotinic receptor silent agonists in human blood immune cells
Name of Candidate Nom du candidat	Espinosa, Eduardo Carlos Soto
Degree Diplôme	Master of Science
Department/Program Département/Programme	Biology
Date of Defence Date de la soutenance	September 03, 2020

APPROVED/APPROUVÉ

Thesis Examiners/Examinateurs de thèse:

Dr. Alain Simard
(Supervisor/Directeur(trice) de thèse)

Dr. Tom Kovala
(Committee member/Membre du comité)

Dr. Alexander Moise
(Committee member/Membre du comité)

Dr. Nader Ghasemlou
(External Examiner/Examinateur externe)

Approved for the Faculty of Graduate Studies
Approuvé pour la Faculté des études supérieures
Dr. Serge Demers
Monsieur Serge Demers
Acting Dean, Faculty of Graduate Studies
Doyen intérimaire, Faculté des études supérieures

ACCESSIBILITY CLAUSE AND PERMISSION TO USE

Abstract

The recent development of α7 nAChR specific molecules, referred to as silent agonists, elicit prolonged channel closing with minimal channel activation and are thought to provoke unique nAChR-dependent metabotropic signaling cascades. This study assessed the anti-inflammatory potential of several silent agonists in modulating lipopolysaccharide (LPS)-induced immune responses in human blood immune cells. Fresh whole blood from healthy volunteers was pre-treated at different time points with silent agonists followed by a 24hr LPS stimulation. Cytometric bead arrays (CBAs) were used to quantify the levels of cytokines IL-1β, IL-6, IL-10, IL-12, and TNF-α in sample supernatants. Then, BioPlex phosphoprotein kits were used to measure phosphorylation levels of various signaling pathway proteins (NF-kB, Akt, ERK1/2, STAT1, and STAT3). For this experiment, peripheral blood mononuclear cells (PBMC) and monocytes isolated from PBMCs were treated with a silent agonist during the LPS stimulation (15-120min). Finally, cell phenotyping studies were carried out in PBMC cultures treated with silent agonists and stimulated with LPS (48hrs). The markers CD14, CD16, CCR2, CD36, CD11c, and HLA-DR were studied. We report that the silent agonist pCF_3 diEPP significantly downregulated the secretion of pro-inflammatory cytokines and phosphorylation of signaling proteins. We did not observe any significant findings with our cell phenotype studies. Overall, our data show that silent agonists modulate LPS-induced release of pro-inflammatory cytokines and signaling events in human peripheral blood immune cells. Silent agonists selective for α7 nAChRs may thus offer a new therapeutic strategy for the treatment of inflammatory diseases.

Keywords

Nicotinic receptors, anti-inflammatory, human blood, silent agonists, novel molecules, immune response, immunology, acetylcholine, drug, flow cytometry, cytokines, signaling, surface marker, treatment.

Abbreviations

AKT	Protein Kinase B
BSA	Bovine Serum Albumin
CNS	Central Nervous System
DMSO	Dimethyl Sulfoxide
EAE	Experimental Autoimmune Encephalomyelitis
ERK1/2	Extracellular Regulated Kinase 1 and 2
FBS	Fetal Bovine Serum
FSC	Forward Scatter
G Mean	Geometric Mean
IL	Interleukin
LPS	Lipopolysaccharide
MS	Multiple Sclerosis
nAChR	Nicotinic Acetylcholine Receptor
NFκB	Nuclear Factor Kappa Light Chain Enhancer of Activated B Cells
pAKT	Phosphorylated Protein Kinase B
PBS	Phosphate Buffered Saline
pERK1/2	Phosphorylated Extracellular Regulated Kinase 1 and 2

PI3K	Phosphoinositide-3-Kinase
pNFκB	Phosphorylated NFκB
PNS	Peripheral Nervous System
pSTAT1	Phosphorylated Signal Transducer and Activator of Transcription 1
pSTAT3	Phosphorylated Signal Transducer and Activator of Transcription 3
SEM	The Standard Error of the Mean
SSC	Side Scatter
STAT1	Signal Transducer and Activator of Transcription 1
STAT3	Signal Transducer and Activator of Transcription 3
TNF-α	Tumor Necrosis Factor alpha

Acknowledgements

I cannot express in words how fruitful my academic journey at the Northern Ontario School of Medicine has been. This project was supervised by Dr. Alain Simard, who is a tremendous scholar, mentor, and friend. Alain made the lab environment warm and inviting, all while facilitating a deeply enriching learning environment. As I continue in the pursuit of scholarly truths, I have no doubt that Dr. Simard will have contributed greatly to my development. For the opportunities given to me, I am forever thankful. I would like to thank Dr. Ramya Narendrula for her dedication and assistance towards the Simard lab. Ramya was always there and happy to lend a hand. We don't know what we'd do without her! I would also like to thank my lab colleagues Max, Maryse, Danika, Gabriella, and Manon, for all the fun times, discussions, and support throughout my time at the Simard lab. They are fantastic to work with and I wish them the best in their future endeavors. For making this study possible, I owe special thanks to phlebotomist Natalie DeSantis for her role in the blood draws, Drs. Papke and Horenstein for their contribution of the silent agonists, and finally, NOSM lab coordinator Natalie Lefort, for her positivity and seemingly knowing how to fix just about anything! We've all been saved by Natalie *at least* once. Finally, I would like to dedicate this thesis to my mother and late father, who shaped me to be the person I am today. Thanks mom and dad.

Table of Contents

List of Figures

List of Tables

1.0 Introduction

1.1.0 The Immune System

Immunology is a broad field concerned with the study of the immune system. The functional role of the immune system is carried out by a series of proteins and cells that collectively elicit an immune response in the presence of foreign invaders or antigens[1]. Such invaders include pathogenic entities such as bacteria, fungi, parasites, proteins, and even cancer cells[2]. Immune cells are found throughout the body, either in discreetly encapsulated organs such as the spleen and thymus, or as dispersed accumulations of lymphoid and myeloid cells in conjunction with the skin and intestine, where they are strategically positioned to control the entry of foreign substances[1]. The environment poses a huge range of potential stimulus to the host, many with unique pathogenic mechanisms of their own[2].

It is then not surprising that the immune system has evolved to possess a vast and complex collection of protective mechanisms to combat the invasion of these foreign invaders[2]. The ability for these protective mechanisms to succeed is strongly reliant on one of the hallmarks of the immune system; that is, to detect structural components on pathogens and toxins that differ from the host cells[2]. Once pathogens are detected, the host immune system will employ several strategies to rid itself from foreign invaders without harming its own cells[2]. These strategies can be simplified into two main categories: Innate immunity and adaptive immunity.

1.1.1 Innate Immunity

Innate immunity is commonly referred to as the first line of defense and is characterized as being a rapid, non-specific, antigen-independent process[2]. Innate immunity is differentiated by its adaptive counterpart in that it lacks immunologic memory[2]. This means that any subsequent exposure to the same antigen will elicit the same response as the first time it was encountered[2]. Examples of innate immunity include anatomical barriers, mechanical removal, inflammatory mediators, activation of complement pathways, phagocytosis, and antimicrobial enzymes and peptides[3]. The removal of foreign entities and cellular debris by the innate response extends to organs, tissues, lymph, and even blood[2].

The presence of microbe-derived pathogen-associated molecular patterns (PAMPs) play important roles in innate immunity. Pattern-recognition receptors (PRRs) expressed on cells can recognize and bind PAMPs and are thus important in triggering the immune response[4]. Examples of prominent PRRs include the Toll-like receptors (TLRs) and the C-type lectin receptors (CLRs)[4]. For the context of this work, TLRs are of special importance. As a type of PRR, TLRs interact with microbial structures such as lipopolysaccharide (LPS), a gram-negative bacterial wall component, but also with cytokines. Such interactions activate inflammatory responses via intracellular signaling pathways MAPK, JAK/STAT, and NF-κB[4].

Ultimately, the innate immune response relies on the orchestration of numerous cells. These cells have been identified as phagocytes, dendritic cells, Natural killer (NK)

cells, basophils, mast cells, and the eosinophils[2]. For the purpose of this study, phagocytes are of interest.

1.1.2 Mononuclear Phagocyte System

Monocytes, macrophages, and dendritic cells (DCs) constitute the mononuclear phagocyte system (MPS)[5]. In particular, both monocytes and macrophages play central roles in the initiation and resolution of inflammation via cytokine release, reactive oxygen species, and phagocytosis of pathogens and dead cells[6]. Before the formation of hematopoietic stem cells (HSCs) *in utero,* monocytes stem from erythro-myeloid precursors in the fetal liver[7,8]. Following birth, monocytes arise from bone marrow-derived HSCs, and are integrated as part of the circulation upon their maturation[9]. Once in the circulation, monocytes survey peripheral tissues and excel at maintaining endothelial integrity[9].

In the presence of pathogenic entities or inflammatory stimuli, monocytes will migrate into tissues and differentiate into macrophages or DCs depending on the surrounding environment[5]. Macrophage activation is achieved by membrane-bound signals and/or secretion of the cytokine IFN-γ via activated T lymphocytes[10]. Once activated, macrophages eradicate intracellular or ingested pathogens[10]. A focus towards monocytes will be discussed for the context of this thesis.

There are two main subsets of monocytes and macrophages that have been extensively studied. They are the classical (inflammatory) and the nonclassical (anti-inflammatory) subsets. In humans, the most abundant are the classical monocytes, making up about 80-95% of circulating monocytes[11]. This subset of monocytes produce

inflammatory cytokines, uses phagocytic action, and are recruited to sites of infection in a rapid manner[11]. They are found in high numbers in the spleen, allowing for their recruitment to the circulation during a systemic inflammatory event[11]. In human samples, such monocytes are characterized by high expression of the marker CD14, lack of CD16, and expression of the chemokine receptor CCR2[11].

The nonclassical subset of monocytes are present in tissues after infection or injury has taken place, and they play a key role in reparative function[11]. Nonclassical monocytes are considered a minority of blood monocytes and are known to patrol along endothelial surfaces[11]. In human samples, they are identified by low expression of the marker CD13, high expression of the marker CD16, and expression of the chemokine receptor CX3CR1[11,12]. Additionally, it has been shown that a third subset in humans exist. This subset is identified by its expression of CD14 and intermediate levels of CD16[13].

1.1.3 Adaptive Immunity

In contrast to innate immunity, adaptive immunity is characterized as being an antigen-dependent and highly specific response[2]. Here, the immune response recognizes and targets non self-antigens from self-antigens (our own cells), thus activating pathogen-specific immunologic effector pathways to eradicate foreign invaders[2]. The most remarkable feature of adaptive immunity lies in its capacity to employ immunological memory, allowing the host to mount a faster and more effective immune response after recurring antigen exposure[2]. The cells of adaptive immunity include T-cells and B-cells, which respectively form the basis of cell-mediated and humoral immunity[3]. Lymphocytes

(such as T and B cells) along with monocytes previously discussed, circulate in the periphery and collectively are known as peripheral blood mononuclear cells (PBMCs).

1.1.4 T cells

T cells are central players in the longevity and stability of the immune response. Such cells have origins as bone marrow progenitors, which migrate to the thymus for purposes of maturation and selection prior to circulation in the periphery[14]. Once in the periphery, T cells establish numerous subsets that include naïve T cells, memory T cells, and regulatory T cells (Tregs)[14]. When a unique type of antigen presenting cell (APC) known as a dendritic cell presents costimulatory ligands, naïve T cells are activated and an immune response begins[14]. This interaction triggers a transcriptional program resulting in the production and release of autocrine/paracrine factor IL-2, which facilitates T cell proliferation[15]. As a consequence of the surrounding cytokine environment, antigen-stimulated T cells will undergo genetic programming into a diverse range of subsets with unique effector mechanisms[15].

Effector T cells are divided primarily into $CD4^+$ helper T cells (Th) and $CD8^+$ cytolytic T cells (CTL)[16]. The T cell receptor of Th cells and CTL cells interact with antigens presented by MHC class II and MHC class I complexes of APCs, respectively[17]. Th cells are categorized into a wide variety of subsets with unique cytokine profiles and functional roles. For instance, Th1 facilitate cell-mediated responses and play key roles in phagocyte-related inflammation[18]. Th1 functions are mediated by their ability to secrete the cytokines IFNγ, IL-2, and TNF[18]. In contrast, Th2 cells are important for humoral immunity and assist in suppressing the activity of phagocytic cells. Much like Th1 cells,

their functions are mediated primarily by the secretion of cytokines IL-4 and IL-10[18]. Th subsets like Th1 have been linked to autoimmune and inflammatory diseases, where their excessive activity facilitates tissue damage and hypersensitivity, respectively[19]. Indeed, methods to modulate cytokine secretion profiles will be of great benefit in modulating immunopathology generated by the dysfunctional activity of such subsets.

1.1.5 B cells

B cells support immune functions in the body and form the basis of humoral immunity. In adults, immature B cells stem from the differentiation of hematopoietic cells in the bone marrow; eventually undergoing development towards the mature form in the spleen[20]. Once matured, B cells have a wide set of functionalities that include antibody secretion, cytokine secretion, and T cell activation via antigen presentation[21]. In particular, the ability of B cells to release cytokines such as IL-1, IL-6, and TNF-α enhance T cell activation, cytokine polarization of Th subsets, and formation of long-lived memory T cells[21]. In contrast, B cell secretion of the anti-inflammatory cytokine IL-10 counteracts T cell activation, regulates the function of innate cells, and prompts an increase of T cells with regulatory activity, thus dampening immune responses[21,22]. In the context of autoimmune and inflammatory diseases, B cells have been implicated for their role in the secretion of aforementioned cytokines; thus like T cells, methods to modulate the secretion of inflammatory cytokines would be advantageous[21].

1.1.6 Intracellular Signaling Pathways

Inflammatory responses require the intricate coordination and activation of signaling pathways that modulate levels of inflammatory mediators in resident tissue

cells and inflammatory cells recruited via the blood[4]. While the inflammatory response is precise to particular stimuli and location within the body, the overall procession can be characterized as such: 1) pattern receptors present on cell surfaces identify harmful stimuli; 2) inflammatory pathways become activated; 3) inflammatory mediators are released; and 4) cells involved in inflammatory responses are recruited to sites of inflammation[4]. The major inflammatory pathways are mitogen-activated protein kinase (MAPK), nuclear factor-κB (NF-κB), Janus kinase/signal transducers and activators of transcription (JAK/STAT), and phosphatidylinositol 3-kinase/protein kinase B (PI3K/Akt). Various studies provide evidence that their dysregulation is associated with inflammatory, autoimmune, metabolic disorders, and cancer[4].

The MAPK pathway constitutes a family of serine/threonine protein kinases that mediate cellular responses to stimuli such as osmotic stress, mitogens, and inflammatory cytokines[4]. Mammalian MAPKs include three major families: extracellular-signal-regulated kinase (ERK1/2), p38 MAP kinase, and c-Jun N-terminal kinases (JNK)[4,23]. Briefly, the ERKs consist primarily of a kinase domain ERK1 and ERK2 which respond to growth factors and mitogens to promote cell growth and differentiation[23]. JNK consist of JNK1, JNK2, and JNK3, which are activated by environmental factors and inflammatory cytokines[23]. JNK activation plays a role in apoptosis, inflammation, cytokine production, and metabolic activity[23]. Activating ERK1/2 and JNK results in the phosphorylation and activation of p38 transcription factors which leads to inflammation, cell cycle regulation, and apoptosis[4,23].

The NF-κB pathway represents a family of inducible transcription factors which function to regulate multiple aspects of innate and adaptive immune responses[24]. There

are five key structurally related members: p50, p52, p65, RelB, and c-Rel, all which supervise transcription of target genes via specific binding to particular DNA elements[24]. Under physiological conditions, NF-κB proteins remain localized in the cytoplasm by members of the IκB family, which have inhibitory roles[24]. NF-κB activation is induced by numerous stimuli, including inflammatory cytokines, enzymes, and pathogen-derived endotoxins such as LPS[4]. Activation signals result in the active state of IκB kinase (IKK), which consists of two kinase subunits, IKKα and IKKβ, and the regulatory subunit IKKγ[4]. IKK modulates NF-κB pathway activation through Iκβ phosphorylation, which prompts the liberation of NF-κB subunits p50 and p65. Site-specific phosphorylation of p65 results in the selective transcription of downstream pro-inflammatory genes, which facilitate the production of pro-inflammatory cytokines[25]. Collectively, this pathway is responsible for inflammatory cytokine production and cell recruitment needed during inflammatory responses[4].

The evolutionarily conserved JAK-STAT pathway functions to mediate cellular responses to numerous cytokines and growth factors[4]. Depending on the signal, such responses include proliferation, differentiation, migration, apoptosis, and cell survival[26]. Currently, four JAKs (JAK1,JAK2,JAK3, and TYK2) and seven mammalian STATs (STAT1,STAT2,STAT3,STAT4,STAT5a,STAT5b, and STAT6) are known[27]. Activation of receptor-associated JAKs via ligand binding leads to their phosphorylation, allowing the formation of STAT docking sites[4]. Following STAT recruitment to these sites, STATs undergo tyrosine phosphorylation and become dimerized[4]. Dimerized STATs translocate to the nucleus where they bind target gene promoter regions and modulate the transcription of inflammatory genes[4].

The PI3K/Akt pathway belongs to a family of lipid kinases that functions to control downstream signaling leading to cytokine production[28,29]. PI3K/Akt is activated by certain toll-like receptors, pathogen recognition receptors, cytokines, and chemokines[29]. Once activated, PI3K type 1 phosphorylates PIP2, resulting in its conversion to PIP3 at the plasma membrane[29]. PIP3 recruits Akt and facilitates its activation via the mechanistic target of rapamycin complex 2 (mTORC2)[29]. Full activation of Akt leads to substrate-specific phosphorylation events throughout the cytoplasm and nucleus; mediating numerous cellular functions such as angiogenesis, metabolism, growth, proliferation, cell survival, protein synthesis, transcription, and apoptosis[30]. An overview of the discussed pathways is represented in **Figure 1**:

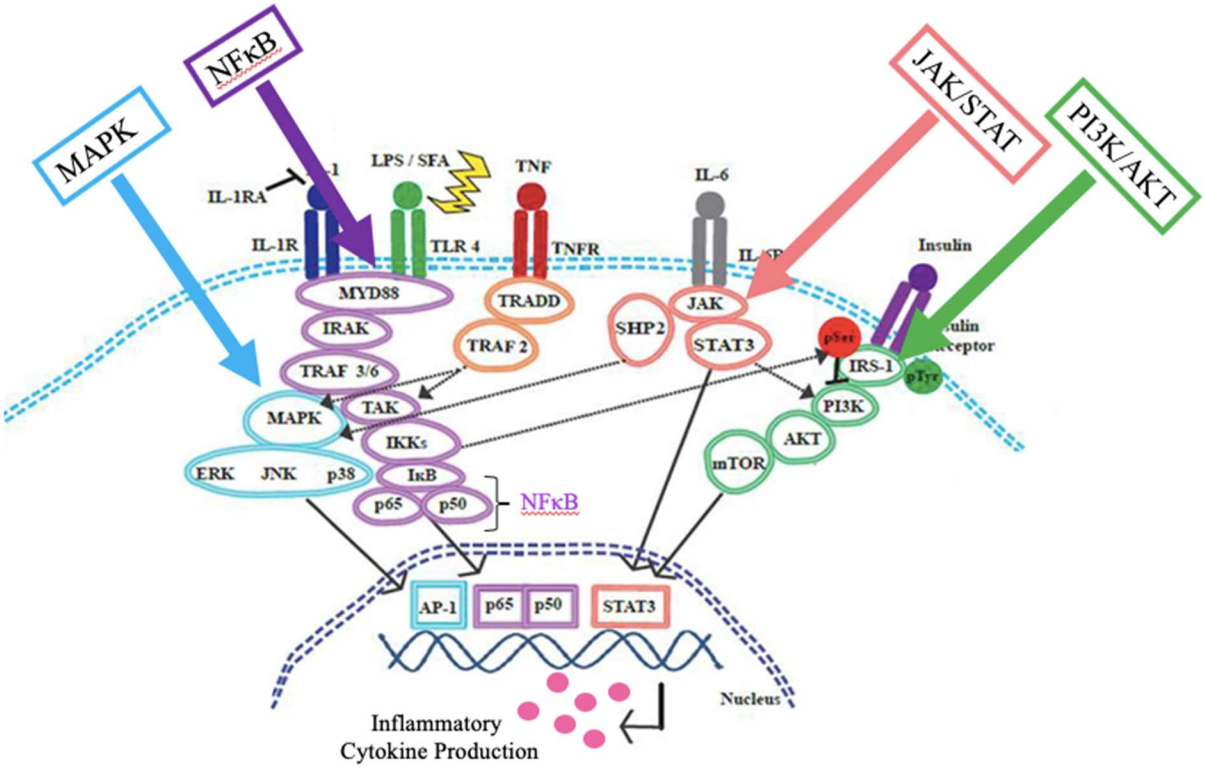

Figure 1: An overview of MAPK, NFκB, JAK/STAT, and PI3K/Akt pathway signaling during inflammation. Modified from Roche *et al.,* 2013.

1.1.7 Cytokines

Cytokines are small, soluble proteins that play a functional role in cell-cell communication and interaction[2]. They are secreted by multiple immune cells, and in particular, by monocytes/macrophages and lymphocytes[31]. Cytokines bind to their receptors on target cells and induce biological responses[17]. Typically, cytokines are released in a cascade fashion, meaning that a single cytokine can cause target cells to produce other cytokines[31]. Cytokine functions are critical for proper immune responses; they prompt the release of various molecules including antibodies, proteins, and

glycoproteins, while facilitating processes such as opsonization, which mediate the engulfment and removal of foreign substances[2]. Cytokines also show redundancy with regards to their function, in that identical activity can be induced by several other cytokines[31].

As key modulators of inflammation, cytokines are divided into two categories: pro-inflammatory and anti-inflammatory. Common pro-inflammatory cytokines include IL-1β, tumor necrosis factor (TNF-α), and IL-6[32]. Such cytokines signal via type I cytokine receptors and are implicated in the mediation of numerous signaling pathways and human disease[32]. Common anti-inflammatory cytokines such as IL-10 function to impede the production of pro-inflammatory cytokines and limit tissue damage to ensure recovery and homeostasis[33].

IL-1β, a highly potent pro-inflammatory cytokine, is expressed by numerous cell types including hepatocytes, monocytes, macrophages and neutrophils[32]. IL-1β release is triggered primarily in response to microbial and viral molecules, which induce pattern recognition receptors (PRRs), toll-like receptors (TLRs), and NOD-like receptors (NLLs)[32]. IL-1β is first synthesized as an inactive precursor, and then is cleaved by caspase-1 (recruited via the inflammasome protein complex) to generate the active form[32]. IL-1R1 and IL-1R2 are two functional IL-1 receptors that, following ligand binding, cue adapter molecule MyD88 to interact with IL-1R1 via its TIR domain, resulting in signal transduction[32]. Consequently, activation of mitogen-activated protein kinases (MAPKs) and the transcription factor NF-κB occurs, leading to pro-inflammatory cytokine expression.

TNF-α is one of the most important and pleiotropic cytokines modulating immune responses[32]. It is secreted by activated macrophages, monocytes, T cells, mast cells, NK cells, and various other cell types[32]. As a type of inflammatory mediator, TNF-α plays a key role in the inflammatory capabilities of the innate immune system, such as cytokine production, adhesion molecule expression, and growth stimulation[32]. In addition, TNF-α exerts cytolytic or cytostatic activity in response to tumor cells, and is implicated in inflammatory, antiviral, and even immunoregulatory action[32]. The two TNF receptors, TNFR1 and TNFR2, promote diverse and opposing biological functions[34]. TNFR1 is expressed by nearly all cell types, while TNFR2 expression is restricted mainly to myeloid cells, lymphocytes (especially Tregs) and certain endothelial cells[35]. Following TNF-α binding to TNFR1, the receptor undergoes internalization which activates an intracellular signaling cascade[32,36]. These signaling events are associated with pro-apoptotic signaling via the formation of complex II (TRADD/FADD/Pro-Caspase-8)[32]. If adaptor molecules are recruited to the cell surface pre-internalization, formation of complex I (TRADD/TRAF2/RIP) occurs and activation of MAPK cascades takes place, leading to transcription factor activation[32,37]. Ultimately, TNFR1 mediates apoptosis and its complex I signaling leads to the expression of pro-inflammatory genes[32,37].

Transmembrane TNF binding to TNFR2 prompts intracellular domains to recruit cytoplasmic TRAF-2-cIAO-1-cIAP-2 complexes, subsequently activating both canonical and non-canonical NF-κB pathways[35]. TNFR2 oversees cell survival in contrast to the apoptotic TNFR1, and is thought to have protective roles in numerous diseases, including those of autoimmune nature[35]. Altogether then, low levels of TNF-α are essential against

pathogens, immune regulation, and suppression of tumor growth; however, the consequence of elevated TNF-α levels results in tissue damage[31].

IL-6 belongs to a family of pleiotropic cytokines and is secreted by various immune cells including phagocytes, T cells, B cells, fibroblasts, bone marrow cells, and some non-immune cells[32]. IL-6 is responsible for numerous immune-related events, such as maturation of B cells into antibody-secreting plasma cells and T cell activation[32]. In addition, IL-6 is a key player in the differentiation and regulation of T-cell helper 2 (Th2) and Treg phenotypes[38,39]. IL-6 acts through its appropriate receptor, the IL-6R α chain (gp80, CD126) found on lymphocytes and hepatocytes, and the gp130 (CD130) component[32]. Classical IL-6R signaling appears to have anti-inflammatory roles, however, gp130 signaling is responsible for the pro-inflammatory activities of IL-6[31]. Thus when IL-6 binds gp130, a signal transduced by the gp130 chains leads to the phosphorylation of the transcription factor STAT3, resulting in its translocation to the nucleus[32]. Once in the nucleus, the transcription of pro-inflammatory genes and intracellular adhesion molecules takes place[32].

IL-10 is an immunomodulatory cytokine secreted by leukocytes such as T helper cells, monocytes, macrophages, dendritic cells, and effector cells such as B cells, NK cells, and granulocytes in response to infection, cancer, or tissue damage[33]. IL-10 elicits immunosuppressive activity via the binding of its respective receptor IL-10R1 and IL-10R2, and while these receptor complexes are found on a wide variety of immune cells, the primary targets of IL-10 are thought to be monocytes and macrophages[33]. Binding of IL-10 to its appropriate receptor facilitates the inhibition of pro-inflammatory mediators and promotes the secretion of the anti-inflammatory IL-1 receptor antagonist (IL-RA),

leading to the inhibition of pro-inflammatory cell development[33]. In addition, IL-10 enhances the activity of Tregs and leads to the activation and proliferation of various immune cells[33,40]. IL-10 has been associated with a therapeutic role in various animal models of disease, such as multiple sclerosis, diabetes mellitus, pancreatitis, and arthritis; however, to what extent remains to be fully realized[33].

1.2.0 Autoimmune Diseases

Autoimmunity is characterized by the immune system orchestrating an attack towards our own cells and tissues (i.e self-cells)[1]. Autoimmune diseases operate through a series of sequential stages, which include initiation, propagation, and resolution[41]. Disease manifestation (initiation) begins as a gradual decline of immunologic tolerance to autoreactive immune cells, and are associated with genetic, infectious, and environmental origins[1]. Next, propagation involves cytokine production, epitope spreading, and an imbalance of effector T-cells and Tregs[41]. Finally, the resolution phase activates both cell intrinsic and extrinsic mechanisms, which activate inhibitory pathways and Tregs, respectively[41]. Patients in the resolution phase often experience relapsing disease events as a result of conflict in controlling pathogenic effector activity and regulation[41]. Given the complex nature of autoimmunity, there are a wide range of diseases and symptoms that are either organ-specific or operate on a systemic basis[1]. Examples include multiple sclerosis, diabetes mellitus, scleroderma, and arthritis[1].

Autoimmune diseases pose a serious threat in clinical settings. Annually they are responsible for a significant portion of healthcare costs, and because of their unusual nature to be prevalent among populations in their prime years, greatly reduce quality of

life[41]. To make matters worse, existing therapies are currently designed such that they address the terminal phase of inflammation, seemingly failing to target the disease at the foundational core responsible for initiation and progression[41]. Consequently, patients suffering from autoimmune diseases have little option but to engage in a life-long treatment process that predisposes them to malignant and infectious complications[41]. While the precise causes of autoimmune pathology remains unknown, tackling such diseases lies in further understanding the source of abnormal immune responses, their maintenance, and the immunological behavior that protects healthy individuals[41]. Thus, current efforts have shifted to developing therapeutic alternatives capable of robust and prolonged disease resolution[41]. In the context of this thesis, one autoimmune disease of interest to us is multiple sclerosis.

1.2.1 Multiple Sclerosis

Multiple Sclerosis (MS) is a chronic autoimmune disorder characterized by the invasion of T- cells, B cells, and macrophages to the central nervous system (CNS); thus encompassing a multifocal inflammatory response[42]. Disease progression of MS is a product of two underlying processes: demyelination associated with failure to remyelinate, and gradual axonal damage with little to no recovery activity[43]. Such responses lead to the formation of inflammatory plaques found in the brain and spinal cord concomitant with astrogliosis and microglia activation[42]. Unsurprisingly, patients with MS and one of its mouse model, experimental autoimmune encephalomyelitis (EAE), experience autonomic and sensorimotor defects which manifest as symptoms that seriously impair quality of life[44]. Examples include difficulty walking, fatigue, visual impairment, ataxia, difficulty thinking, and numerous others[44]. Unfortunately, MS affects

mostly young adults plagued with predisposing genetic and environmental factors that are believed to set the stage for disease initiation and subsequent progression[45].

The underlying cause of MS remains unclear, however it is known that following the invasion of activated immune cells to the CNS, these cells release cytokines which contribute to disease pathology[32,46]. Specifically, patients with MS show elevated levels of TNF-α in active lesions of the CNS, the periphery, and in the cerebrospinal fluid[31]. In addition, concentrated levels of IL-6 have been reported in active MS plaques, and is thought to control the balance between Th17 and Tregs[31,47]. Finally, levels of IL-10 are found to be reduced in MS patients, and in animal models, IL-10 deficiency was shown to induce a stronger and accelerated inflammatory response[32,48]. Studies targeting cytokines involved in MS pathology will be critical in the development of therapeutic strategies.

1.2.2 Current Therapeutics

Therapeutic options for patients with MS are very limited, with roughly 15 approved drugs by the FDA available[49]. To make matters worse, not all treatment plans work for patients and many have unwanted side effects such as insomnia, increased blood pressure, mood swings, fluid retention, flu-like symptoms, skin irritation, and reduced ability to fight infection[49]. Current MS therapies attempt to reduce the inflammatory responses by targeting pathways such as β-interferons, IFNβ-1α, and IFNβ-1β; others modulate lymphocyte trafficking and differentiation[42]. Current drugs focus primarily on amelioration of the secondary progressive form[50]. Treatment of the secondary progressive form helps to reduce both the rate of disease relapse and neurological disability[50].

While most of the focus in MS pathogenesis is widely attributed to lymphocyte activity of the adaptive immunity, in particular autoreactive CD8+ and CD4+ T cells, the involvement of myeloid cells remains shockingly overlooked[51].

1.2.3 Role of Myeloid Cells in MS

Myeloid cells is an encompassing term used to describe monocytes, macrophages, dendritic cells, and microglia[51]. Indeed, it was found that myeloid cells are the primary immune cells in current and persistent MS plaques, and remain in advanced secondary MS[51]. This observation is linked to the capacity of myeloid cells to secrete a wide range of inflammatory cytokines, free radicals, and proteases[51]. Coupled with lymphocyte activity, myeloid cells facilitate an inflammatory milieu that augments the demyelination process[51]. That said, myeloid cells are also crucial for employing repair mechanisms that promote disease recovery[52].

This seemingly contradictory function of myeloid cells is attributed to an existing spectrum of monocyte/macrophage phenotypes commonly divided into two core subsets: M1 and M2 cells[53]. Human M1 cells (classically activated), are stimulated by the cytokine IFN-γ and the gram-negative bacterial membrane component, lipopolysaccharide (LPS)[51]. M1 cells express high levels of costimulatory molecules CD80 and CD86, which are important for antigen presentation efficiency[54]. M1 cells upregulate TLR2, TLR4, MHC-II, chemokine receptor CCR7, and generate the production of several chemokines including C-C motif ligand 2 (CCL2) and C-X-C motif ligand 10 (CXCL10)[55]. Once in their active state, M1 cells secrete high levels of nitric oxide and the pro-inflammatory cytokines IL-1β, IL-12, IL-23, and TNF-α[51].

Collectively, these secretion products coordinate the induction of pro-inflammatory Th1/17 cells and contribute to disease pathology resulting in tissue damage[12,13].

Human M2 cells (alternatively activated) are activated by local tissue damage, promote Th2-type responses, and are associated with anti-inflammatory and regulatory activity, thus enabling repair mechanisms and subsequent disease recovery[15,16,17]. Key biological markers of this population include CD23, the scavenger receptors CD163/CD204, and the mannose receptor CD206[54]. M2 cells represent a broader set of responses compared to their M1 counterparts and can be further divided into three activation states: M2a, M2b, and M2c[57].

Briefly, M2a macrophages secrete polyamines and IL-10, which cease the activity of pro-inflammatory cytokines generated by M1 cells[57]. M2b macrophages promote selective up-regulation of phagocytosis and regulate the inflammatory response, while M2c subsets are important for tissue repair, extracellular matrix repair, and the dampening of M1/Th1 immune responses[57]. Collectively, the three M2 activation states work to establish healing/reparative responses, and function to oppose their pro-inflammatory M1 counterparts[57]. An overview of these functions can be seen in **Figure 2** below:

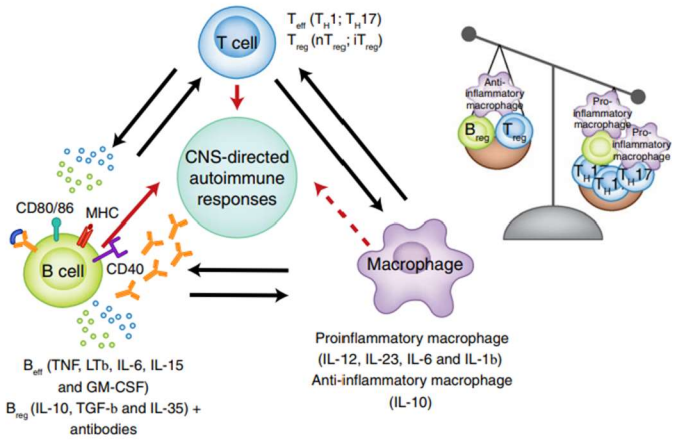

Figure 2: The emerging view of myeloid cell involvement in MS pathology
Various cell subsets and their products are shown[58]. Modified from Li *et al.,* 2018.

A study working with EAE, a mouse model for MS, reported that modulating the balance between M1 and M2 cells during the early clinical phase determines the severity of disease in EAE[55]. Remarkably, the study reached two conclusions: 1) M2 cell markers appeared to be suppressed in the neuroinflammatory responses associated with EAE and 2) Therapeutic administration of M2-activated cells in the ongoing first clinical phase attack showed suppression of relapsing in EAE[55]. Taken together, this suggests a novel and concise objective: to discover and employ molecules that restore M2 cell populations[55].

1.3.0 Nicotinic Acetylcholine Receptors

Acetylcholine receptors (AChRs) can be divided into two major subtypes: the muscarinic receptors and the ionotropic nicotinic receptors[59]. Both receptors are activated by acetylcholine (ACh), a type of endogenous neurotransmitter[59]. Nicotinic acetylcholine

receptors (nAChR) are a class of ligand-gated ion channels belonging to the superfamily of Cys-loop receptor channels[60]. Nicotinic receptors can exist as five different subunits, including α, β, δ, and γ (fetal) or ε[61]. Different subtype combinations manifest as receptors with unique pharmacological properties. In the mammalian brain, genes encoding α (α2- α10) and β (β2- β4) have been identified[60,62]. Functional nAChRs structurally consist of a five-subunit arrangement into homomeric or heteromeric channels that facilitate the transport of Na^+, K^+, and Ca^{2+} ions across plasma membranes[60].

In 1970, the nAChR was the first neurotransmitter receptor to be isolated and purified from the electric organs of the fish *Electrophorus electricus* and *Torpedo*[63]. Structurally, cryo-electron microscopy of the nAChR revealed a transmembrane cylinder; its long axis perpendicular to the membrane[63]. From a top-view, the pentameric subunits are formed around a central pore and are thought to resemble a rosette-like arrangement[63]. Individual subunits contain four hydrophobic transmembrane domains termed M1 through M4, a short extracellular C-terminus, a long extracellular N-terminal, and a characteristic cytoplasmic loop between M3 and M4[64]. Subunits are categorized as α or non-α subunits[59]. An overview of the nAChR subunit structure and arrangement is shown in **Figure 3**:

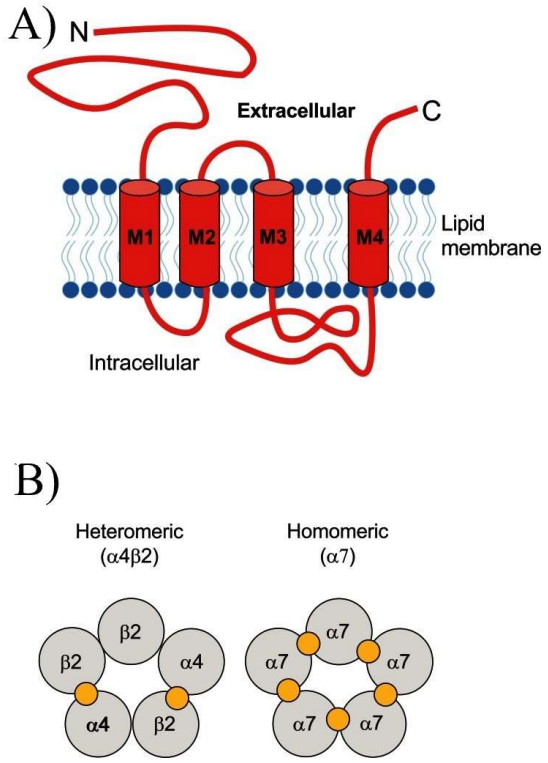

Figure 3: Structure and composition of neuronal nAChRs

(**A**) nAChRs consist of five subunits individually having a large amino-terminal extracellular domain, hydrophobic transmembrane domains denoted M1-M4, and a large intracellular loop[65]. (**B**) The pentameric nAChR subunits may be arranged in a heteromeric (i.e α4β2) or homomeric (i.e α7) fashion. The yellow circles represent the binding site of the neurotransmitter acetylcholine. Modified from Ceña *et al.,* 2013.

A key feature of α subunits is based on the presence of a Cys-Cys pair, which is found near the entrance to M1 and is functionally responsible for agonist binding[59]. Studies dedicated to the binding kinetics of nicotinic ligands and rapid kinetic measurements of ion-channel opening/closing have revealed that nAChRs behave as allosteric proteins[63]. This implies that the binding site and ion channels are spaced far from each other and can undergo reversible transitions between unique allosteric conformations in the presence or absence of agonists[63].

In the central nervous system (CNS) of mammalian models, nAChRs are expressed in the presynaptic neuronal membrane where they regulate the release of neurotransmitters[61]. In the peripheral nervous system (PNS), expression of nicotinic receptors are mostly post-synaptic and important for rapid synaptic transmission[61]. Altogether, nicotinic receptors play key roles in numerous processes, including neuromuscular signaling, learning, memory, and reward pathways[62]. The recent discovery that nAChRs are expressed in nonneuronal cells of the body, particularly in immune cells, have led to the suggestion that nAChRs play key roles in immune processes. α7 nicotinic receptors are among the most abundant of nAChRs and are found on both neuronal and non-neuronal cells such as immune cells, astrocytes, microglia, oligodendrocyte precursor cells, and endothelial cells[66]. Among the numerous subtypes of nAChRs, the α7 subtype has been the subject of much work within the context of inflammation.

For example, molecules such as nicotine and acetylcholine acting on the α7 nAChR subtype have been shown to confer protective effects against EAE[67], which is characterized by the invasion of immune cells, primarily M1, into the CNS[68]. Th2 and Treg cells normally protect against autoimmunity by promoting tolerance of self-antigens; however, in the EAE model their functions are suppressed during the initial stages of disease[69]. Studies report that nicotine exposure to α7 nAChRs reduces the infiltration of pro-inflammatory M1-induced Th1/Th17 cells in the CNS during EAE and impedes the destruction of myelin and axons by increasing the reactivity of Th2 and Treg cells[68].

Moreover, experiments involving septic shock rat models using LPS further found that acetylcholine and nicotine binding to α7 nAChRs significantly decreased the LPS-induced release of TNF-α from cultured human macrophages, but failed to do so in α7-KO mice[70]. A study using primary cultures of murine bone marrow cells found that nicotine administration inhibited the increase of IFNγ-induced pro-inflammatory monocytes by reducing cell proliferation and viability[71]. The same study showed that nicotine inhibited the production of pro-inflammatory cytokines TNF-α, IL-1β, and IL-12 and promoted the secretion of the anti-inflammatory cytokine, IL-10[71]. Taken together, these findings suggest that α7 nAChRs have an essential role in the regulation of inflammation.

In addition to the above, this subtype is characterized by its high Ca^{2+} permeability, rapid desensitization, low probability of channel opening, and seemingly ubiquitous expression on various immune cells, making it an ideal therapeutic target[64]. Recently, Thomsen and Mikkelson showed that increased α7 ion channel currents via binding of agonists and positive allosteric modulators (PAMs) failed to reduce the production of LPS-induced pro-inflammatory cytokines such as TNFα, while those that acted as very weak partial agonists showed clear dose-dependent reductions of TNF production[72]. These findings suggests that ionotropic action is not involved in the anti-inflammatory properties of α7 nAChRs; instead, anti-inflammatory action is a consequence of α7 nAChR interaction with non-activating ligands that prompt a metabotropic mode of operation[73].

Upon binding of agonists and subsequent activation, nAChRs will experience allosteric transition, a conversion from a closed, resting state to that of an open state[74].

Once in the open state, an influx of Na^+ (and some Ca^{2+}), and an efflux of K^+ ions takes place, leading to membrane depolarization and the transmission of signals at cholinergic synapses[75,76]. Within seconds or minutes after agonist binding, the nAChR channel closes, entering what is called a desensitised state[75].

In the desensitised state (**Figure 4**), the receptor retains binding capability with increased agonist affinity, but the agonist itself will cease to induce ion channel activation[76]. Previously, ion channel opening was thought to be associated with the anti-inflammatory and disease modifying capabilities of nAChRs, however, increasing evidence suggests that such protective action is instead a consequence of prolonged channel closing via desensitization[77].

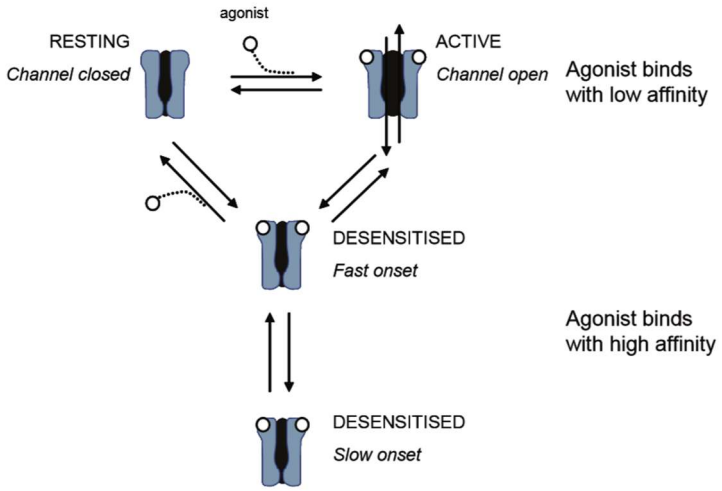

Figure 4. The proposed conformational states of nAChRs and their relationship
Modified from Wonnacott & Barik, 2007 [78].

1.3.2 α7 nAChR Signaling

In non-neuronal cells, anti-inflammatory properties of α7 nAChRs appear to be due primarily to the inhibition of the NF-κB pathway, although the extent to which this is achieved is not entirely clear[79–81]. One model reports that α7 nAChRs are coupled to JAK2 and STAT3, which upon acetylcholine or nicotine binding of the receptor, become activated[64]. Perhaps the most prominent mechanism by which α7 nAChRs modulate NF-κB signaling involves the JAK/STAT pathway. Here, the binding of cholinergic agonists to the α7 nAChR recruits Jak2 to the receptor, followed by the autophosphorylation of JAK2[64]. Phosphorylated JAK2 then recruits and phosphorylates STAT3, leading to STAT3 dimerization and subsequent translocation to the nucleus where it forms protein-protein interactions with NF-κB and inhibits the transcription of pro-inflammatory genes[64]. In a separate 2011 study, Joe *et al.* suggest that STAT3 may not be primarily responsible for the anti-inflammatory activities of the JAK/STAT pathway; instead, anti-inflammatory effects are caused by STAT3-induced production of tristetraprolin (TTP)[82]. Since TTP is an AU-rich element (ARE) binding protein, experiments using the monocytic cell line, U937, showed that TTP could destabilize pro-inflammatory transcripts possessing AREs at the 3'-untranslated region[82].

Other groups propose that inhibition of STAT3 phosphorylation is responsible for the anti-inflammatory component of α7 nAChR signaling. In this model, α7 nAChR activation promotes unphosphorylated STAT3 (uSTAT3), which interacts with NF-κB subunits p50/p65 in the cytoplasm and prevents NF-κB nuclear translocation[83].

Since NF-κB is necessary in the transcription of various pro-inflammatory cytokine genes such as IL-1β, IL-6, and TNF-α, this proposed pathway ultimately enables the suppression of pro-inflammatory activity[64]. Interestingly, numerous studies report that signaling via α7 nAChRs does not appear to alter or inhibit the production of anti-inflammatory cytokines[84]. The proposed signaling mechanism via α7 nAChRs is shown in **Figure 5**.

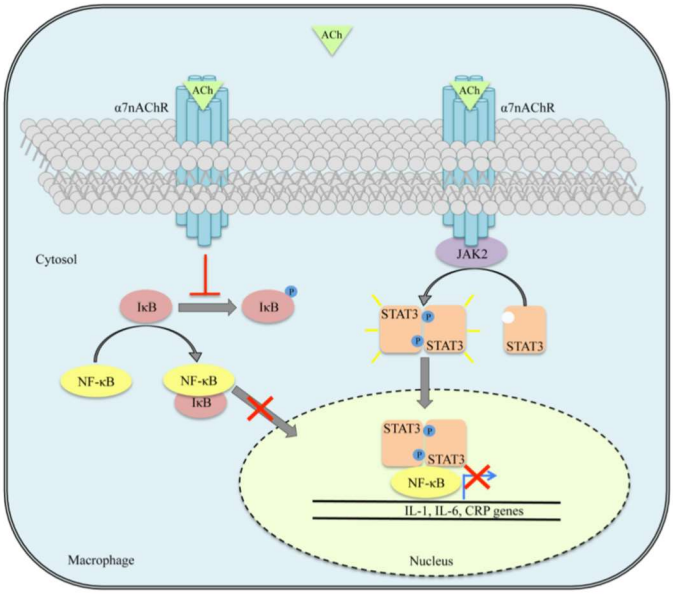

Figure 5: Binding of α7 nAChRs by acetylcholine on splenic macrophages inhibits NF-κB activity, thus transcription of pro-inflammatory cytokine genes is suppressed. In this model, splenic nerve activation leads to the release of norepinephrine, which binds to β2 adrenergic receptors on choline acetyl transferase (ChAT) expressing T-cells, prompting the synthesis and release of acetylcholine. Modified from Cuoco *et al.,* 2016.

Beyond NF-κB and JAK/STAT pathways, studies further suggest that α7 nAChRs modulate the MAPK and PI3K/Akt pathways. For example, a study working with various α7 nAChR-selective agonists in PC12 cells endogenously expressing α7 nAChRs showed a dose-dependent increase in the MAPK pathway component, ERK1/2[85]. In addition, the

study suggests that α7 nAChR agonist-triggered intracellular Ca^{2+} transients in PC12 cells lead to the activation of calmodulin-dependent protein kinase II, which prompts phosphorylation of p38 MAPK, MEK1/2, and ERK1/2[85]. In the presence of α7 nAChR competitive antagonist methyllycaconitine or chelation of extracellular Ca^{2+}, the effect of α7 nAChR agonism was attenuated, suggesting that ERK1/2 pathway activity is mediated by the ionotropic functions of the nAChRs[85].

Regarding the PI3K/Akt pathway, a study working with normal human bronchial epithelial cells and small airway epithelial cells showed that nicotine was able to induce Akt phosphorylation in a time and dose-dependent manner, along with downstream substrates[86]. Others working with both neuronal and non-neuronal cells found that α7 nAChR agonists also trigger phosphorylation of Akt via Jak2 and PI3K activation[80]. Contrary to these findings however, Yue *et al.,* showed that in LPS-stimulated RAW264.7 cells, the selective α7 nAChR agonist GTS-21 significantly reduced Akt phosphorylation levels in a dose-dependent manner and aided with the suppression of LPS-induced inflammation[87]. Finally, a group working with LPS-stimulated RAW264.7 cells reported that α7 activation via nicotine suppressed LPS-induced TLR4 overexpression through the PI3K/Akt pathway and may indeed reprogram macrophages to become refractory and hyporesponsive to TLR activation[64].

1.3.3 Silent Agonists

In line with the previous mentioned observation that ionotropic action is not involved in the anti-inflammatory properties of α7 nAChRs, the task of developing molecules that are selective for the α7 nAChR and do not stimulate its ionotropic activity

may be of great therapeutic potential[73]. In this regard, the emergence of a new class of molecules called silent agonists have been the subject of recent study. Silent agonists are unique molecules that are "silent" in the ionotropic sense, but are "agonists" such that if you co-apply them with a positive allosteric modulator, they induce channel opening[73]. More specifically, silent agonists are very weak α7-selective partial agonists that produce little to no channel activation on their own[88], but possess the ability to induce prolonged states of desensitization[89]. As previously mentioned, the desensitized state is an altered conformational state thought to promote metabotropic signaling cascades responsible for the anti-inflammatory capabilities of these receptors[77].

In relation to other nAChR subtypes, silent agonists do not appear to bind the majority of heteromeric nAChRs[90]. Interestingly, it remains to be determined if silent agonists can bind the highly expressed homomeric α9 nAChR and what functional implications they may hold for this subtype. However, the current lack of reliable tools limits the extent to which this can be addressed.

The α7-selective silent agonists analyzed in this project were m-bromo PEP, m-$CONH_2$ diEPP iodide, m-$CONH_2$ diEPP bromide, and p-CF_3 diEPP. These molecules were synthetically developed by Dr. Papke and Dr. Horenstein from the University of Florida. Although numerous derivatives of silent agonists have been produced in recent years, the above four silent agonists were chosen because 1) they have the most selectivity to α7 nAChRs and 2) they show the least ionotropic activity when applied alone, while still being able to induce channel opening when a positive allosteric modulator is co-applied.

While few studies involving silent agonists exist, recent work has shown these molecules to be quite effective with *in vitro* and *in vivo* models of inflammation. A study using the α7-selective silent agonist NS6740 proved to be more efficacious than other α7 agonists in the attenuation of LPS-induced TNF-α release in microglial cells[72]. In addition, Papke *et al.,* demonstrated that NS6740 indeed had anti-inflammatory and reparative effects in several mouse models of disease[77]. Furthermore, a recent study showed that one of the DEPP-based analogues, formerly known as m-bromo PEP was able to downregulate IL-6 and TNF-α after a 6-hour LPS stimulation[91]. m-bromo PEP could also protect against EAE by decreasing the infiltration of macrophages, T-cells, and B-cells to the CNS[91]. Such findings imply a promising role for silent agonists in a therapeutic context, however, further work is needed to understand how these molecules modulate α7-related signaling events in different cell types and organ systems[77]. **Figure 6** shows the structure of the silent agonists used in this study:

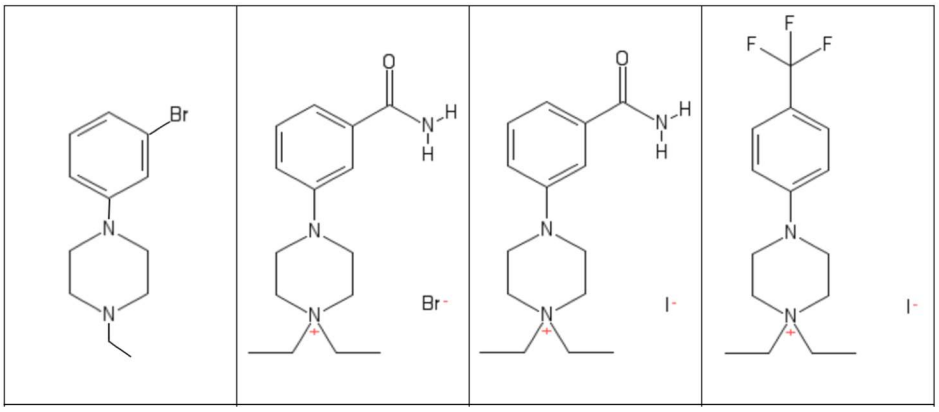

m-bromo PEP m-$CONH_2$ diEPP Bromide m-$CONH_2$ diEPP Iodide p-CF_3 diEPP

Figure 6: Structure of silent agonists
The silent agonists m-bromo PEP, m-CONH2 diEPP Bromide, m-CONH2 diEPP Iodide, and p-CF3 diEPP. Drug molecules were synthesized and obtained from the Department of Chemistry, University of Florida. Courtesy of Drs. Horenstein and Papke.

2.0 Objectives & Hypothesis

This study set out to determine the extent to which various α7 nAChR-selective silent agonists could modulate inflammatory responses by human blood immune cells. As LPS is known to activate signaling pathways MAPK, NF-kB, PI3K/Akt, JAK/STAT, promote the transcription of pro-inflammatory cytokine genes, and influence cell phenotype characteristics, we hypothesize that α7 nAChR-selective silent agonists will counteract these LPS-induced effects.

3.0 Materials & Methods

Chemicals

Silent agonists were synthesized as previously described[92] and arrived as pure crystalline products. Molecules were stored at -20°C until ready to use. Stock solutions of m-bromo PEP, m-CONH2 diEPP bromide, m-CONH2 diEPP iodide, and PCF3 diEPP were prepared at 100mM in dimethylsulfoxide (DMSO) and were further diluted to 10mM in phosphate buffered saline (PBS). Antagonist molecules methyllycaconitine, tubocurarine chloride, COG133, and mecamylamine hydrochloride were received as crystalline products and diluted to 10mM stock solutions in DMSO. Molecules were prepared fresh each day at the desired concentration from the stored stock solution.

3.1.0 Cytokine Secretion Profiles

3.1.1 Participants

Participants were individuals over the age of 18 who do not smoke tobacco and do not routinely take anti-inflammatory medications. Exclusion criteria includes donors with known inflammatory disorders and recent or ongoing infections. To minimize variability, participants were required to fast 10 hours prior to blood donation. Experiments were reviewed, approved, and performed in accordance with the policies outlined by the Laurentian University Research Ethics Board for Research Involving Human Participants.

3.1.2 Collection of Blood Samples

Human blood was acquired per participant via a licensed phlebotomist. To prevent blood clotting, 10 x 10mL (up to 100mL total) blood samples were collected in BD Vacutainer™ glass blood collection tubes containing sodium heparin (BD, Cat#B366489) and were individually shaken periodically during and after the blood draw. Care was taken to minimize time required to process samples.

3.1.3 Whole Blood Preparation

200uL of heparinized whole blood was added to wells of a tissue culture treated Costar® 24-well flat-bottom plate (Stemcell, Cat#38017). Whole blood was diluted in either 700uL or 800uL of Sigma RPMI-1640 medium with L-glutamine and sodium bicarbonate (Sigma, Cat#R8758).

3.1.4 Pre-treatments & Stimulation

Wells containing RPMI-diluted whole blood were pre-treated with 10uL of 10mM silent agonists to achieve a working concentration of 100uM for 1 and 24 hours at 37°C. To wells not pre-treated with silent agonists, 10uL 0.1% DMSO (Sigma, Cat#D2650) was added as a control. Following pre-treatment time points, wells were stimulated with 100uL of LPS at a working concentration of 100ng/mL (eBioscience, Cat#L500497693) for 24 hours at 37°C. For controls, wells not treated with LPS received 100uL of RPMI-1640 medium.

To determine the mechanisms responsible for our cytokine profile observations, an additional set of wells were co-treated with 10uL of one of each 10mM antagonist (Table 1) and 10uL of 10mM silent agonists to achieve a working concentration of 100uM for 1 and 24 hours at 37°C (**Table 1**). Following pre-treatment time points, wells were then stimulated with 100uL of 100ng/mL LPS for 24 hours at 37°C. For controls, wells were treated with antagonist alone or with LPS using the previously mentioned conditions. Additional controls included a well with no treatment and a well stimulated with LPS only.

Table 1: Antagonists and their respective functional characteristics

Function	Antagonists
α7 selective Antagonist	Methyllycaconitine (APExBIO, Cat#B6556)
Competitive nAChR Antagonist	Tubocurarine Chloride (Tocris, Cat#2820/50)
α7 Non-competitive Antagonist	COG133 (APExBIO, Cat#A1131-10)
Non-competitive nAChR Antagonist	Mecamylamine hydrochloride (APExBIO, Cat#B7205-10)

3.1.5 Cytokine Collection & Storage

Following the 24-hour LPS stimulation, the contents of each well was transferred to a 1.5mL Eppendorf tube and centrifuged at 20,000g for 5 minutes at room temperature. Supernatants containing cytokines were then collected and transferred to pre-labeled Eppendorf tubes. Samples were stored at -20°C until ready to use.

3.1.6 Preparation of Cytokine Standard Curves

Lyophilized standards were obtained for cytokines of interest: Human IL-1β Flex kit (BD Biosciences, Cat#558279), Human IL-6 Flex kit (BD Biosciences, Cat#558276), Human IL-10 Flex kit (BD Biosciences, No. 558274), and Human TNF Flex kit (BD Biosciences, Cat#560112). The manufacturer's *Preparing Human Flex Set Standards* protocol was followed to generate the standard curves.

3.1.7 BD Cytometric Bead Array (CBA)

The manufacturer's protocol found in the *BD Cytometric Bead Array (CBA) Human Soluble Protein Master Buffer Kit Instruction Manual* was followed. 50uL of supernatant sample was diluted in 450uL of 1X PBS (Fischer Scientific, Cat#BP399-500) to achieve a 1/10 dilution. 25uL of diluted sample was then transferred to BD Falcon™ FACs tubes (BD, Cat#352008). For the designated negative control, no supernatant sample was added.

Capture beads master mix were prepared using the 50X capture bead stock vials from each flex kit and 1X PBS. Stock vials were diluted with 1X PBS such that the

capture bead master mix ensured a volume of 25uL per FACs tube containing supernatant sample. 25uL of capture bead master mix was then added to each sample and mixed well by pipetting. Tubes were then incubated at room temperature in the dark for one hour. Following incubation, the detection antibodies master mix was prepared using the same steps outlined earlier. 25uL of detection antibodies master mix was added to each tube and mixed well by pipetting. Tubes were then incubated at room temperature in the dark for two hours.

Following incubation, tubes were washed with 1mL of 1X PBS and centrifuged at 230g and 4°C for 5 minutes. The supernatant was discarded, and the samples were analyzed via flow cytometry.

3.1.8 Flow Cytometry

Flow cytometry was performed on a BD FACS Canto II flow cytometer in conjunction with BD FACS Diva Software (v6.1.3). For voltage (V) parameters, the flow cytometer was calibrated routinely and tested to ensure proper readings. For each sample, 2000 events were acquired. Data obtained was further interpreted using FCAP Array Software (v3.0).

3.1.9 Statistical Analysis

Due to the high variability from blood donors immune system[77], a sample size (n) of 20 was determined through power analysis to complete the study. The data was normalized by setting the concentration of each cytokine obtained from the LPS + DMSO treatment condition to 100% and calculating all other values accordingly. Data was

analyzed by repeated measures (RM) one-way ANOVA with multiple comparisons using Dunnett's correction. Treatments were compared to the LPS+DMSO group (*: $P \leq 0.05$; **: $P \leq 0.01$, ***: $P \leq 0.001$, ****: $P \leq 0.0001$). Results are always presented as means ± S.E.M. Statistical analysis was performed on GraphPad Prism 8.4.1 software.

3.2.0 Cell Signaling Studies

3.2.1 PBMC Isolation

Peripheral blood mononuclear cells were isolated following SepMate protocols. Fresh PBS + 2% FBS (Gibco, Cat#10082147) and complete medium (RPMI-1640 + L-glutamine medium, 10% FBS) were prepared prior to starting. Briefly, 100mL of whole blood was diluted in equal volume of PBS + 2% FBS and mixed. Next, 15mL of lymphocyte separation medium (Corning, Cat#MT25072CV) was added to a determined number of SepMate™-50 tubes (Stemcell, Cat#85460). 34mL of diluted whole blood was added to each SepMate™-50 tube to allow for mixing with the separation medium above the insert. Tubes were centrifuged at 1200g for 10 minutes at room temperature.

Following centrifugation, the top layer containing enriched mononuclear cells was collected in 50mL centrifuge tubes (Basix, Cat#14955238) and filled to the 50mL mark with PBS + 2% FBS. Samples were centrifuged at 300g for 8 minutes at room temperature. The majority of supernatant was removed from each tube, and the pellets were resuspended and combined into one 50mL centrifuge tube. PBS+2% FBS was added to the 50mL mark, and the previously mentioned centrifugation settings were used. The supernatant was removed, and the pellet was resuspended in 3-10mL of 1X RBC lysis buffer for 4-5 minutes. Following a series of centrifugation and washing steps,

PBMCs were resuspended in 5mL of complete medium and stored in ice until ready to use.

3.2.2 Monocyte Isolation

Monocytes were isolated from PBMCs using the MACS Pan Monocyte Isolation kit protocol (Miltenyi Biotec, Cat#130-096-537). Complete medium and MACs separation buffer was prepared using 100mL PBS+0.5% BSA, 2mM EDTA prior to starting experiments. Following PBMC isolation, total PBMC cell number was determined, and cells were centrifuged at 300g for 8 minutes at room temperature. After removing the supernatant, cells were resuspended in 40uL of MACS separation buffer per 10^7 total cells. 10uL each of FcR blocking reagent and biotin-antibody cocktail were added to the cell suspension per 10^7 total cells, mixed, and incubated for 5 minutes at 4°C. Following incubation, 30uL of MACS separation buffer and 20uL of anti-biotin microbeads were added to the cell suspension per 10^7 total cells and incubated for 10 minutes at 4°C.

For magnetic separation, a MidiMACS Separator (Miltenyi Biotec, Cat#130-042-302) was attached to a MACS MultiStand (Miltenyi Biotec, Cat#130-042-303) and a LS column (Miltenyi Biotec, Cat#130-042-401) was inserted into the separator. A 15mL conical tube (FisherSci, Cat#14955238) was placed underneath the LS column, and the column was rinsed with 3mL of MACS separation buffer. A new tube was placed underneath the column and the cell suspension was applied to the column. Flow through containing enriched monocytes was collected. Further washing steps were taken and collected in the same tube. Using FACS analysis, monocyte purity was evaluated by

fluorescent staining with APC anti-human CD14-phycoerythrin (PE) monoclonal antibody (BioLegend, Cat#325608) and was found to always be above 90%.

3.2.3 Stimulation

Condition	(A)	(B)	(C)	(D)	(E)	(F)
Stimuli	---	---	---	LPS	LPS	LPS
Drug Treatment	---	DMSO	pCF3 DiEPP	---	DMSO	pCF3 diEPP

PBMC and monocyte suspensions were centrifuged at 350g for 8 minutes at room temperature. Supernatants were removed and re-suspended in a volume of pre-warmed complete medium (37°C) required to reach $1x10^6$ cells/mL. Cells were then separated in respective tubes representing different conditions (**Table 2**). To activate signaling pathways of interest, cells were stimulated with LPS, yielding a final concentration of 100ng/mL. Cells were then treated with silent agonists and DMSO were at a final working concentration of 100uM and 0.1%, respectively. Tubes were then incubated at 37°C for 30 minutes.

Table 2: Different treatment conditions for PBMC and monocyte-enriched cells
Controls include a negative control (A), DMSO only (B), Silent agonist only (C), positive control (D), and LPS with DMSO only (E).

3.2.4 Cell Lysis

Tubes containing cells were pelleted at 1000g for 5 minutes at 4°C following the incubation period. Cells were then resuspended in ice-cold wash buffer and pelleted with the above parameters. To lyse cells, a pre-calculated amount of cell lysis buffer containing protease inhibitor phenylmethylsulfonyl fluoride at a working concentration of

2mM (PMSF) (BioRad, Cat#171304006M) and HALT complete protease inhibitor cocktail at a 1X working concentration (ThermoFisher, Cat#78446) was added to cells in each tube. Tubes were gently rocked for 20 minutes at 4°C and stored away at -80°C until ready to use. The suggested working protein concentration range for Bio-Plex® cell signaling assays is 2–200 μg/ml

3.2.5 BCA Assay

To ensure the required working protein concentration range, the Pierce™ BCA Protein Assay Kit (ThermoFisher, Cat#23225) was used following the manufacturer's microplate instructions. 1X PBS and lysis buffer were used for the protein blanks. Plates were analyzed using the BioTex PowerWave XS plate reader (Serial #198303) and absorbances were read at a 562nm wavelength for each well of the plate using Gen 5 software (v2.0).

3.2.6 Phosphoprotein Measurement

To study phosphorylation events in our pathways of interest, the Bio-Plex cell signaling kit was used. All assay components were brought to room temperature and prepared fresh on the day of experiment. Cell lysates and controls were thawed and centrifuged at 15,000g for 10 minutes at 4°C. Next, a master mix from 20x stock coupled beads (Table 3) was prepared using manufacturer calculations. 25uL of master mix was added to each well of a Bio-Plex Pro™ flat bottom plate (BioRad, Cat#171025001). The plate was then placed on the Bio-Plex Pro™ handheld magnetic washer (BioRad, Cat#171020100) and wash steps were performed following manufacturer's instructions. Next, 25uL of cell lysates, as well as positive (TNF-α and IFN-α) and negative

(Phosphatase) control cell lysates, were added to wells containing coupled beads. The plate was covered with a sheet of adhesive foil (ThermoFisher, Cat#AB0626) and loaded on a plate shaker set to 330 RPM for 15-18 hours at room temperature.

Following the incubation period, a series of washing steps were performed and a master mix from 20x detection antibodies was prepared using manufacturer calculations. 12.5uL of the detection antibody master mix (**Table 3**) was added to the appropriate wells of the plate and covered. The plate was then loaded on a plate shaker set to 330 RPM for 30 minutes at room temperature. Following incubation and washing steps, 100x stock of SA-PE was diluted to 1X. 25uL of Diluted SA-PE was added to appropriate wells, covered, and shaken at 330 RPM for 10 minutes at room temperature. After the time period, 62.5uL of resuspension buffer was added to each well of the plate and covered. The plate was shaken at 900 RPM for 30 seconds, and the contents of each well was transferred over to FACS tubes.

Table 3: Bio-Plex Pro Magnetic Cell Signaling Assays

Bio-Plex Phosphoprotein Assay	Target Site
NF-κB p65 (BioRad, Cat#171-V50013M)	Ser^{536}
ERK1/2 (BioRad, Cat#171-V50006M)	Thr^{202}/Tyr^{204}, Thr^{185}/Tyr^{187}
Akt (BioRad, Cat#171-V50001M)	Ser^{473}
STAT1 (BioRad, Cat#171-V50020M)	Tyr^{701}
STAT3 (BioRad, Cat#171-V50022M)	Tyr^{705}

3.2.7 Flow Cytometry

Flow cytometry was performed on a BD FACS Canto II flow cytometer in conjunction with BD FACS Diva Software (v6.1.3). For voltage (V) parameters, the flow cytometer was calibrated routinely and tested to ensure proper readings. For each sample, 1500 events were acquired. Data obtained was further analyzed on Kaluza software (v2.1.1).

3.2.8 Statistical Analysis

A power analysis conducted on GPower v3.1.9.4 gave us a pre-determined n of 12 and 11 for PBMCs and monocytes respectively (α=0.05, d=0.8) to achieve a power of .80. Since this study is one of the first to be conducted, there were no previously published human blood experiments resembling this one, and so the data used for the power analysis originated from our preliminary results of our first three samples.

Data was analyzed using the Geometric mean fluorescence of intensity (G mean) of each protein. The G mean is a measure of central tendency commonly used with flow cytometric data to establish the fluorescence of the antibody bound to a phosphorylated protein, allowing us to measure phosphorylation levels of that protein. An increase or decrease in the G mean fluorescence intensity of a phosphoprotein indicates an upregulation or downregulation of phosphorylation, respectively. G means for each treatment condition were then normalized using B-Actin housekeeping protein. Fold

change was determined by comparing each treatment group to the no treatment group. The average of these fold changes was obtained and presented for each phosphoprotein.

Data is presented as means of fold change ± SEM and was analyzed by RM one-way ANOVA with multiple comparisons using Dunnett's correction. The LPS + DMSO group was used as the comparative control (*: $P \leq 0.05$; **: $P \leq 0.01$, ***: $P \leq 0.001$). Statistical analysis was performed on GraphPad Prism 8.4.1 software.

3.3.0 Cell Phenotype Studies

3.3.1 Cell Culture

Following isolation of PBMCs, cells were diluted in complete medium to reach a concentration of $1x10^6$ cells/mL. 3mL of cell suspension was added to each well of a 6-well plate for a total of $3x10^6$ cells per well.

3.3.2 Stimulation

Cells were treated with silent agonists and DMSO at a working concentration of 100uM and 0.1%, respectively. Wells not pre-treated with silent agonist received DMSO as a control. To induce an inflammatory response, wells were stimulated with LPS, yielding a final concentration of 100ng/mL. Cells were incubated at 37°C for 48hrs. Wells containing only DMSO and silent agonist were used as controls.

3.3.3 Detachment

Following incubation, supernatant from each plate well was transferred to respective 15mL conical tubes. To detach macrophages from the wells, wells were flushed with 1mL of 1X TrypLE^{TM} Express Enzyme (Gibco, Cat#12604021). Plates were then gently shaken and incubated at 37°C for 20 minutes. Following incubation, wells were flushed with 2mL RPMI and the contents of each well was transferred to aforementioned 15mL conical tubes. Tubes were then centrifuged at 530g for 15 minutes at 4°C and 1mL of supernatant was left to resuspend. To count cells, cells were diluted (1:5) in trypan blue and 20uL was loaded between a hemocytometer and cover glass. Under a microscope, the cells in all four outer squares of the loaded hemocytometer were counted and the mean number of cells was obtained.

3.3.4 Antibody Staining

Cell suspension was taken from each respective tube and transferred to individual wells of a 96-well plate. Cells were diluted with 1X PBS to reach a concentration of 600,000 cells/mL. The plate was then centrifuged at 250g for 2 minutes at 4°C. A calculated volume of Fc Blocker (BD, Cat#564220) was added to each well and incubated at 4°C for 15 minutes. During incubation, an antibody master mix for surface markers of interest (Table 4) was prepared following manufacturer's instructions. 20uL of antibody master mix was added to each well and gently shaken. The plate was covered with aluminum foil and incubated at 4°C for 35 minutes. Following incubation, 220uL of PBS was added to each well and the plate was spun at 250g for 2 minutes at room

temperature. Supernatant was discarded and contents of wells were transferred to labeled FACs tubes.

Table 4: Antibodies used for flow cytometric analysis.

Target	Conjugate	Clone	Host	Source
CD14	APC-Cy7	HCD14	Mouse	BioLegend, Cat#325620
CD16	PE	3G8	Mouse	BioLegend, Cat#302008
CD36	FITC	5-271	Mouse	BioLegend, Cat#336204
CCR2	APC	K036C2	Mouse	BioLegend, Cat#357208
HLA-DR	PerCP-Cy 5.5	G46-6	Mouse	BD, Cat#552764
CD11c	PE-Cy 7	B-ly6	Mouse	BD, Cat#561356

3.3.5 Flow Cytometry

Cells were analyzed on a BD FACS Canto II flow cytometer (BD, #Y96100029) in conjunction with BD FACS Diva Software (v6.1.3), measuring 50,000 events. Negative controls were included. The voltage parameters were routinely calibrated, and data obtained was further analyzed on Kaluza software (v2.1.1). To remove doublets, the data was first plotted as FSC-area versus FSC-height, followed by the placement of a gate in the dense region of the plot. A second plot, gating from the population in the first plot, was plotted as SSC-area versus FSC-area, and defined cell populations were further gated to remove debris from the analysis.

3.3.6 Statistical Analysis

A pre-determined n value of 20 was determined using a power analysis with data originating from previously published experiments (data not shown) and is on the higher side due to increased variability in human immune systems. **Due to complications with the project, a final n value of 18 was achieved.** Data is presented as means ± S.E.M and was analyzed by RM one-way ANOVA with multiple comparisons using Dunnett's correction (*: $P \leq 0.05$; **: $P \leq 0.01$, ***: $P \leq 0.001$). Statistical analysis was performed on GraphPad Prism 8.4.1 software.

4.0 Results

The current project investigated the role of silent agonists in modulating LPS-induced responses in human blood immune cells. To determine how silent agonists modulate cytokine profiles in human whole blood, we used cytometric bead array techniques to measure LPS-induced cytokine levels in the presence of varied silent agonists. We next sought to define whether the silent agonists could modulate pro-inflammatory pathways of interest in both PBMCs and monocyte-specific cells. To do this, protein phosphorylation was quantified for a series of pathway proteins using a Bio-Plex Pro cell signaling assay. Finally, to determine the extent by which silent agonists can influence M1/M2 cell phenotyping, PBMCs were stimulated with LPS and cultured for 48hrs. Cells were stained for numerous markers of interest and analyzed via flow cytometry.

4.1.0 Silent agonists decrease IL-6 secretion in LPS-treated human whole blood

As expected, 1hr pre-treatment of cells was observed to substantially decrease the percent of cytokine secretion between the LPS+DMSO comparative group versus the LPS+ pCF_3 diEPP group (100% vs 79±7%, P=0.0095, n=20). 24hr pre-treatment of cells with the same silent agonist did not appear to decrease IL-6 secretion (100% vs 122±25%, P=0.7800, n=20). Preliminary findings involving 1hr and 24hr pre-treatments of cells with the silent agonists m-bromo PEP (100% vs 146±19%; 99±9%, n=10), m-$CONH_2$ diEPP bromide (100% vs 93±20%; 133±25%, n=8), and m-$CONH_2$ diEPP iodide (100% vs 122±32%; 73±15%, n=8) did not appear to decrease IL-6 secretion versus the LPS + DMSO comparative group. As seen in **Figure 7A**, 1hr pre-treatments with the silent agonist pCF_3 diEPP significantly downregulated LPS-induced secretion of the cytokine IL-6 in human whole blood. In contrast, 24hr pre-treatments did not significantly modulate IL-6 expression (**Figure 7B)**. Descriptive statistics for all silent agonists and treatment conditions are summarized in **Table 5**:

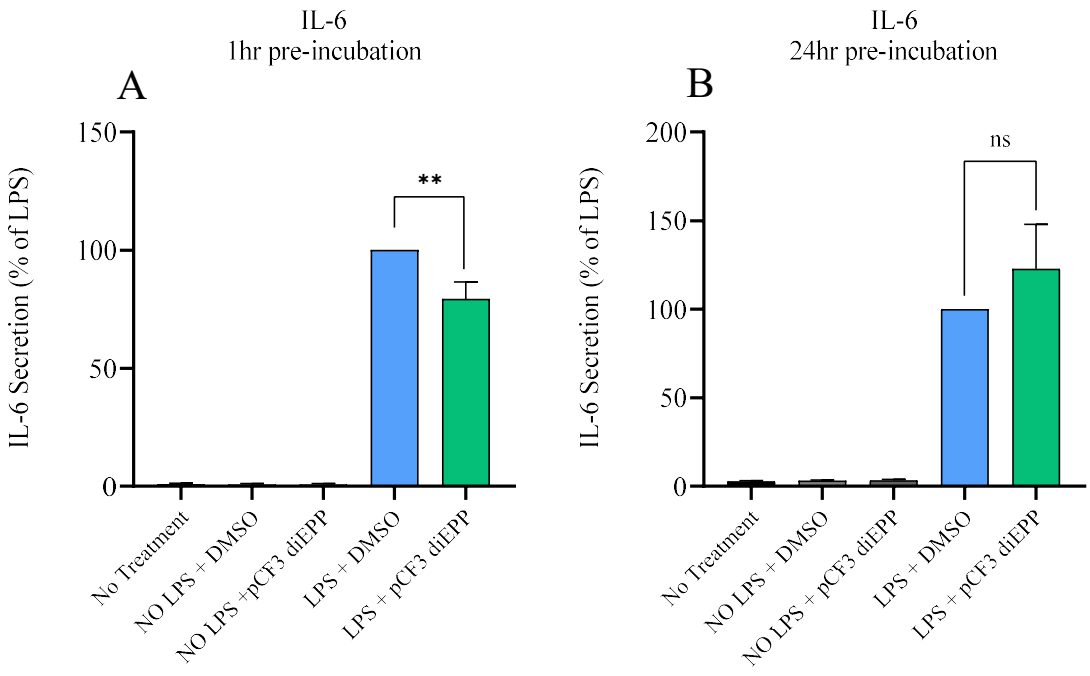

Figure 7: The silent agonist pCF_3 diEPP decreases LPS-induced IL-6 secretion in human whole blood Blood from healthy donors was obtained. Whole blood was pre-treated with a working concentration of 100 µM silent agonists for 1hr or 24hr, followed by a 24hr LPS stimulation. To quantify cytokine secretion, CBA assay kits were used in conjunction with flow cytometry. The data was normalized by setting the concentration of IL-6 obtained from the LPS + DMSO group alone to 100% and calculating all other values accordingly (A) LPS (100ng/mL) induced secretion of IL-6 in human whole blood was measured in the presence of the silent agonist pCF_3 diEPP pre-treated for 1hr. 1hr pre-treatment with pCF_3 diEPP significantly downregulated LPS-induced IL-6 secretion. (B) LPS (100ng/mL) induced secretion of IL-6 in human whole blood was measured in the presence of the silent agonist pCF_3 diEPP pre-treated for 24hr. 24hr pre-treatment with pCF_3 diEPP failed to downregulate LPS-induced IL-6 secretion. The symbol * denotes statistically significant findings between the indicated treatment and the LPS+DMSO comparative group (*: $P \leq 0.05$; **: $P \leq 0.01$, ***: $P \leq 0.001$) using RM one-way ANOVA, Dunnett's multiple comparisons test.

Table 5: Descriptive statistics of IL-6 expression showing the mean, SEM, and sample size (n)

IL-6	Pre-treatment	m-bromo PEP		m-$CONH_2$ diEPP Bromide		m-$CONH_2$ diEPP Iodide		pCF3 diEPP	
		Mean ± SEM	n	Mean ± SEM	n	Mean ± SEM	n	Mean ± SEM	n
No Treatment	1hr	0.8±0.4	15	0.8±0.4	15	0.8±0.4	15	0.8±0.4	15
	24hr	2±0.4	15	2±0.4	15	2±0.4	15	2±0.4	15
LPS + DMSO	1hr	100	10	100	8	100	8	100	20
	24hr	100	10	100	8	100	8	100	20

LPS + Silent agonist	1hr	146±19	10	93±2	8	122±32	8	79±7	20
	24hr	99±9	10	133±25	8	73±15	8	122±25	20
DMSO Only	1hr	0.2±0.2	10	0.2±0.1	8	0.3±0.1	8	0.8±0.4	20
	24hr	6±4	10	9±6	8	21±19	8	3±0.5	20
Silent agonist Only	1hr	0.2±0.1	10	0.2±0.1	8	0.3±0.2	8	0.8±0.3	20
	24hr	8±5	10	10±7	8	15±13	8	3±0.5	20

4.1.1 Silent agonists decrease IL-1β secretion in LPS-treated human whole blood

For 1hr pre-treatments, a strong decrease in percent of IL-1β secretion for the LPS+DMSO comparative group versus the LPS+pCF_3 diEPP group (100% vs 65±5%, P=<0.0001, n=20) was observed. At 24hr pre-treatments, a modest decrease in IL-1β secretion was seen between the LPS+DMSO comparative group and the LPS+ pCF_3 diEPP group (100% vs 87±5%, P=0.2983, n=20). Preliminary findings involving 1hr and 24hr pre-treatments with the silent agonists m-bromo PEP (100% vs 136±19%; 95±4%, n=10) and m-$CONH_2$ diEPP iodide (100% vs 104±20%; 91±18%, n=8) did not appear to decrease IL-1β secretion following LPS stimulation. Though no statistical conclusion could be made, a 1hr pre-treatment of the silent agonist m-$CONH_2$ diEPP bromide appeared to show a decreasing trend between the LPS+DMSO comparative group and the LPS+m-$CONH_2$ diEPP bromide treated group (100% vs 75±13%, n=8), but did not appear to do so after a 24hr pre-treatment (100% vs 97±8%, n=8). As seen in **Figure 8A**, 1hr pre-treatment of cells with the silent agonist pCF_3 diEPP significantly downregulated LPS induced secretion of the cytokine IL-1β in human whole blood. In **Figure 8B**, 24hr pre-treatment of cells with pCF_3 diEPP did not significantly modulate IL-1β secretion. Descriptive statistics for all silent agonists and treatment conditions are summarized in **Table 6**:

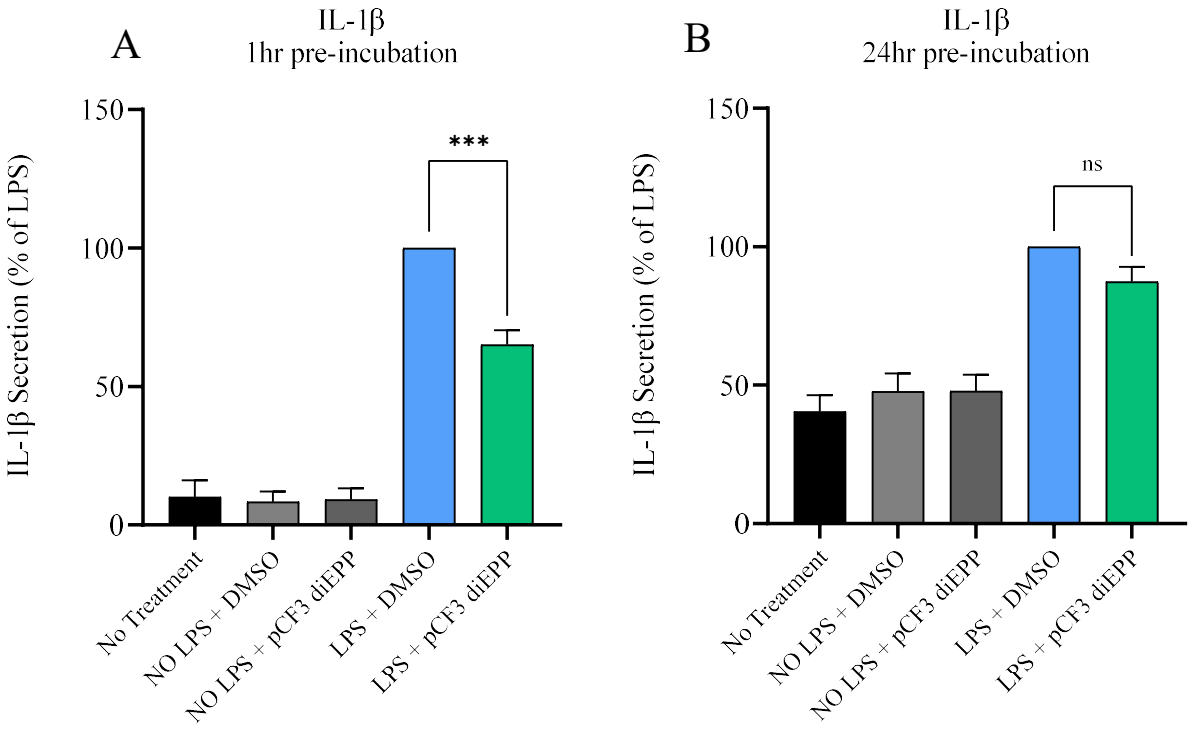

Figure 8: The silent agonist pCF_3 diEPP decreases LPS-induced IL-1β secretion in human whole blood Blood from healthy donors was obtained. Whole blood was pre-treated with a working concentration of 100 μM silent agonists for 1hr or 24hr, followed by a 24hr LPS stimulation. To quantify cytokine secretion, CBA assay kits were used in conjunction with flow cytometry. The data was normalized by setting the concentration of IL-1β obtained from the LPS + DMSO group alone to 100% and calculating all other values accordingly. (A) LPS (100ng/mL) induced secretion of IL-1β in human whole blood was measured in the presence of the silent agonist pCF_3 diEPP pre-treated for 1hr. 1hr pre-treatment with pCF_3 diEPP significantly downregulated LPS-induced IL-1β secretion. (B) LPS (100ng/mL) induced secretion of IL-1β in human whole blood was measured in the presence of the silent agonist pCF_3 diEPP pre-treated for 24hr. 24hr pre-treatment with pCF_3 diEPP showed a modest, non-significant decrease in LPS-induced IL-1β secretion. The symbol * denotes statistically significant findings between the indicated treatment and the LPS+DMSO comparative group (*: $P \leq 0.05$; **: $P \leq 0.01$, ***: $P \leq 0.001$) using RM one-way ANOVA, Dunnett's multiple comparisons test.

Table 6: Descriptive statistics of IL-1β expression showing the mean, SEM, and sample size (n)

IL-1β	Pre-treatment	m-bromo PEP	m-$CONH_2$ diEPP Bromide	m-$CONH_2$ diEPP Iodide	pCF3 diEPP

		Mean ± SEM	n	Mean ± SEM	n	Mean ± SEM	n	Mean ± SEM	n
No Treatment	1hr	10±6	15	10±6	15	10±6	15	10±6	15
	24hr	40±5	15	40±5	15	40±5	15	40±5	15
LPS + DMSO	1hr	100	10	100	8	100	8	100	20
	24hr	100	10	100	8	100	8	100	20
LPS + Silent agonist	1hr	136±19	10	75±13	8	104.6±20	8	65±5	20
	24hr	95±4	10	97±8	8	91±18	8	87±5	20
DMSO Only	1hr	3±1	10	4±1	8	4±2	8	8±3	20
	24hr	49±9	10	58±9	8	54±14	8	47±6	20
Silent agonist Only	1hr	3±1	10	4±1	8	5±2	8	9±4	20
	24hr	52±9	10	61±10	8	55±16	8	47±5	20

4.1.2 Silent agonists decrease TNF-α secretion in LPS-treated human whole blood

For 1hr pre-treatments, a strong decrease in percent of cytokine secretion was observed with PCF_3-diEPP-treated samples versus the LPS+DMSO comparative group (100% vs 62±9%, P=<0.0007, n=20). 24hr pre-treatments with PCF_3-diEPP did not appear to reduce LPS-induced TNF-α secretion as seen from the LPS+DMSO comparative group (100% vs 104±11%, P=0.9881, n=20). Preliminary findings involving 1hr and 24hr pre-treatments respectively with the silent agonist m-bromo PEP (100% vs 101±23%; 85±10%, n=10) did not appear to modulate TNF-α secretion versus the LPS+DMSO comparative group. In contrast, 1hr-pretreatments with the silent agonist m-$CONH_2$ diEPP bromide showed a modest decrease of TNF-α (100% vs 85±18%, n=8), while m-$CONH_2$ diEPP iodide (100% vs 64±13%, n=8) appeared to strongly decrease TNF-α secretion. The effect seemingly reversed at 24hr pre-treatments. As seen in **Figure 9A**, 1hr pre-treatments with the silent agonist PCF_3-diEPP significantly inhibited the secretion of the cytokine TNF-α in human whole blood stimulated with LPS. **Figure 9B** shows that 24hr pre-treatments did not significantly reduce LPS-induced TNF-α

secretion from the LPS+DMSO comparative group versus the LPS+pCF$_3$ diEPP group. Descriptive statistics for all silent agonists and treatment conditions are summarized in **Table 7**:

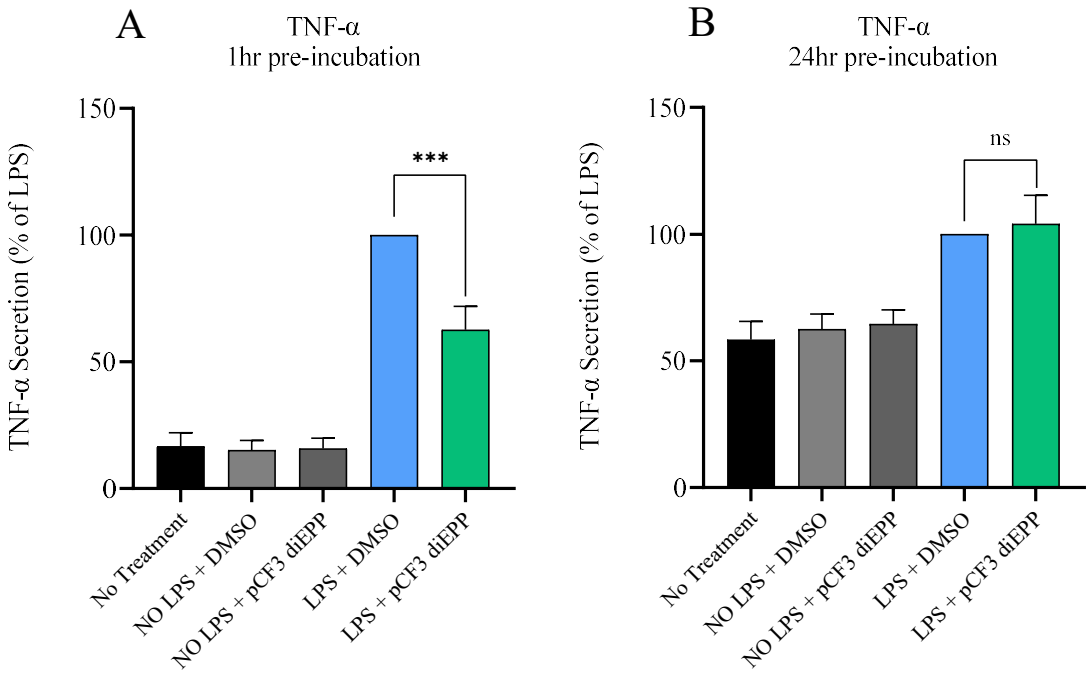

Figure 9: The silent agonist pCF$_3$ diEPP decreases LPS-induced TNF-α secretion in human whole blood Blood from healthy donors was obtained. Whole blood was pre-treated with a working concentration of 100 µM silent agonists for 1hr or 24hr, followed by a 24hr LPS stimulation. To quantify cytokine secretion, CBA assay kits were used in conjunction with flow cytometry. The data was normalized by setting the concentration of TNF-α obtained from the LPS + DMSO group alone to 100% and calculating all other values accordingly. (A) LPS (100ng/mL) induced secretion of TNF-α in human whole blood was measured in the presence of the silent agonist pCF3 diEPP pre-treated for 1hr. 1hr pre-treatment with pCF3 diEPP significantly downregulated LPS-induced TNF-α secretion. (B) LPS (100ng/mL) induced secretion of TNF-α in human whole blood was measured in the presence of the silent agonist pCF3 diEPP pre-treated for 24hr. 24hr pre-treatment with pCF3 diEPP did not modulate LPS-induced TNF-α secretion. The symbol * denotes statistically significant findings between the indicated treatment and the LPS+DMSO comparative group (*: $P \leq 0.05$; **: $P \leq 0.01$, ***: $P \leq 0.001$) using RM one-way ANOVA, Dunnett's multiple comparisons test.

Table 7: Descriptive statistics of TNF-α expression showing the mean, SEM, and sample size (n)

TNF-α	Pre-treatment	m-bromo PEP		m-$CONH_2$ diEPP Bromide		m-$CONH_2$ diEPP Iodide		pCF3 diEPP	
		Mean ± SEM	n	Mean ± SEM	n	Mean ± SEM	n	Mean ± SEM	n
No Treatment	1hr	16±5	15	16±5	15	16±5	15	16±5	15
	24hr	58±7	15	58±7	15	58±7	15	58±7	15
LPS + DMSO	1hr	100	10	100	8	100	8	100	20
	24hr	100	10	100	8	100	8	100	20
LPS + Silent agonist	1hr	101±23	10	85±18	8	64±13	8	62±9	20
	24hr	85±10	10	116±36	8	96±18	8	104±11	20
DMSO Only	1hr	12±4	10	10±3	8	12±3	8	22±5	20
	24hr	39±6	10	60±8	8	64±9	8	62±5	20
Silent agonist Only	1hr	8±3	10	11±3	8	12±3	8	27±6	20
	24hr	35±7	10	58±9	8	55±9	8	64±5	20

4.1.3 Silent agonists do not modulate IL-10 secretion in LPS-treated human whole blood

At both 1hr and 24hr pre-treatments, a minute decrease in percent IL-10 secretion was observed with the LPS + DMSO comparative group versus the LPS + pCF_3 diEPP group respectively (100% vs 91±4%, P=0.0875, n=20; 100% vs 96±13%, P=0.9984, n=20). Interestingly, 1hr pre-treatment with the silent agonist m-bromo PEP appeared to modestly increase IL-10 secretion during the LPS stimulation, though the effects seemingly reversed at 24hr pre-treatment (100 vs 119±11; 85±10, n=10, respectively). The silent agonist m-$CONH_2$ diEPP bromide did not seem to modulate secretion levels of IL-10 at either 1hr or 24hr pre-treatment points, respectively (100 vs 97±13%; 100% vs 91±14%, n=8). Unexpectedly, 1hr and 24hr pre-treatments with the silent agonist m-$CONH_2$ diEPP iodide was observed to moderately decrease levels of IL-10 secretion versus the comparative group (100% vs 80±11%; 100% vs 70±10%, n=8, respectively).

Shown in **Figure 10**, treatment with the silent agonist pCF_3 diEPP did not significantly modulate the levels of the anti-inflammatory cytokine IL-10 in LPS-stimulated human whole blood. Descriptive statistics for all silent agonists and treatment conditions are summarized in **Table 8.**

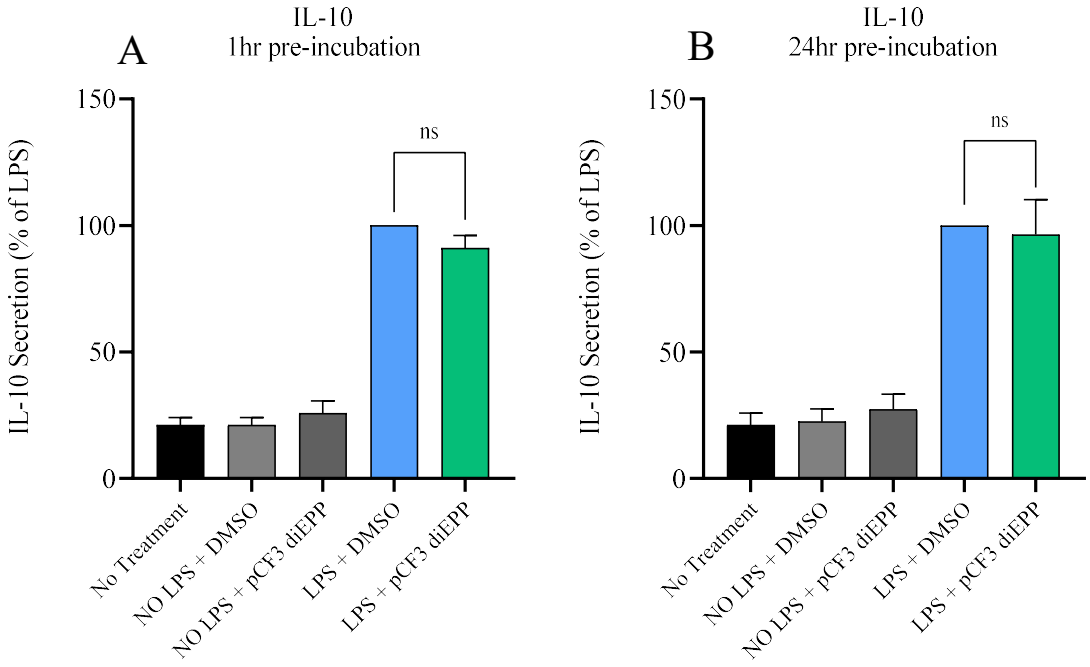

Figure 10: The silent agonist pCF_3 diEPP does not modulate LPS-induced IL-10 secretion in human whole blood Blood from healthy donors was obtained. Whole blood was pre-treated with 100 µM silent agonists for 1hr or 24hr, followed by a 24hr LPS stimulation. To quantify cytokine secretion, CBA assay kits were used in conjunction with flow cytometry. The data was normalized by setting the concentration of IL-10 obtained from the LPS + DMSO group alone to 100% and calculating all other values accordingly. **(A)** LPS (100ng/mL) induced secretion of IL-10 in human whole blood was measured in the presence of the silent agonist pCF_3 diEPP pre-treated for 1hr. 1hr pre-treatment with pCF_3 diEPP did not modulate LPS-induced IL-10 secretion. **(B)** LPS (100ng/mL) induced secretion of IL-10 in human whole blood was measured in the presence of the silent agonist pCF_3 diEPP pre-treated for 24hr. 24hr pre-treatment with pCF_3 diEPP did not modulate LPS-induced IL-10 secretion. The symbol 'ns' denotes non-significant findings between the indicated treatment and the LPS+DMSO comparative group using RM one-way ANOVA, Dunnett's multiple comparisons test.

Table 8: Descriptive statistics of IL-10 expression showing the mean, SEM, and sample size (n)

IL-10	Pre-treatment	m-bromo PEP		m-$CONH_2$ diEPP Bromide		m-$CONH_2$ diEPP Iodide		pCF3 diEPP	
		Mean ± SEM	n	Mean ± SEM	n	Mean ± SEM	n	Mean ± SEM	n
No Treatment	1hr	20±3	15	20±3	15	20±3	15	20±3	15
	24hr	21±4	15	21±4	15	21±4	15	21±4	15
LPS + DMSO	1hr	100	10	100	8	100	8	100	20
	24hr	100	10	100	8	100	8	100	20
LPS + Silent agonist	1hr	119±11	10	97±13	8	80±11	8	91±4	20
	24hr	99±5	10	91±14	8	70±10	8	96±13	20
DMSO Only	1hr	20±4	10	22±5	8	23±5	8	21±3	20
	24hr	25±9	10	21±4	8	29±10	8	22±5	20
Silent agonist Only	1hr	28±9	10	32±12	8	36±12	8	25±4	20
	24hr	30±10	10	32±11	8	32±13	8	27±6	20

4.1.4 Silent agonist pCF3 diEPP modulated LPS-induced phosphorylation of NFκB p65 in PBMCs

When compared to the no treatment control group, treatment with LPS alone was observed to strongly increase NFκB p65 phosphorylation (1.0 vs 2.8±0.2, P=0.0002, n=13). As expected, treatment with the silent agonist pCF_3 diEPP prior to LPS stimulation was found to decrease the levels of NFκB p65 phosphorylation (2.8 ± 0.2 vs 2.0 ± 0.2, P = 0.0215, n=13). Treatments with pCF_3 diEPP alone (0.9±0.08, n=13) or DMSO alone (1.0±0.04, n=13) did not appear to show any apparent deviation when compared to the no-treatment group. As seen in **Figure 11**, LPS-induced NFκB p65 phosphorylation (pNFκB p65) in peripheral blood mononuclear cells was significantly diminished in the presence of the silent agonist pCF_3 diEPP.

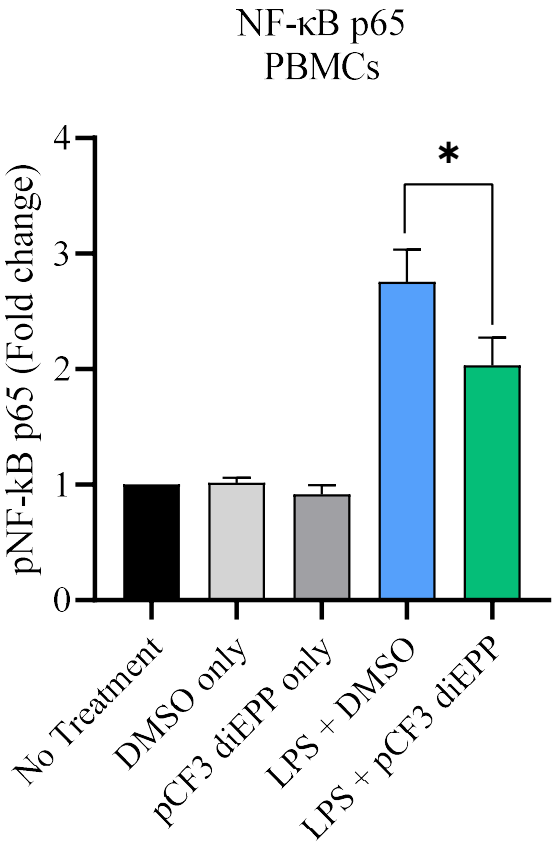

Figure 11: The silent agonist pCF_3 diEPP-modulated phosphorylation of NFκB p65 in the presence of LPS stimuli Following the collection of human whole blood, peripheral blood mononuclear cells were isolated and separated into 5 different conditions. Respective conditions were stimulated with LPS (100 ng/mL) for 30 minutes, in the presence of 0.1% DMSO or pCF_3 diEPP at a concentration of 100 µM. For controls, PBMC samples were treated with pCF_3 diEPP alone or with 0.1% DMSO alone. The no treatment condition served as a baseline for the fold change of pNFκB p65. The α7 nAChR silent agonist pCF_3 diEPP-modulated phosphorylation of NFκB p65. The cell culture supernatant was analyzed by performing a Bio-Plex Phosphorylation Assay followed by FACS analysis. LPS increased pNFκB p65 levels, while pCF_3 diEPP significantly decreased pNFκB p65 levels, as observed in the reduction in fold change between the LPS + DMSO and LPS + pCF_3 diEPP conditions. Data shown are fold change means ± SEM (n= 13). The symbol * denotes statistically significant findings between the LPS + pCF_3 diEPP treatment and LPS + DMSO comparative group (*: $P \leq 0.05$; **: $P \leq 0.01$, ***: $P \leq 0.001$) using a RM one-way ANOVA, Dunnett's multiple comparisons test.

4.1.5 Silent agonist pCF3 diEPP modulated LPS-induced phosphorylation of STAT1, STAT3, AKT, and ERK1/2 in PBMCs

STAT1, STAT3, AKT, and ERK1/2 were the remaining proteins studied. For all proteins, LPS stimulation was observed to slightly increase their phosphorylation. Pre-treatment with pCF_3 diEPP weakly decreased LPS-induced phosphorylation of the aforementioned proteins. For controls (No treatment, DMSO only, and pCF_3 diEPP only) all phosphoproteins studied here showed similar trends as seen with pNFκB p65. All proteins displayed similar trends, such that LPS stimulation appeared to slightly increase their phosphorylation, while pre-treatment with pCF_3 diEPP seemingly reduced phosphorylation levels. The extent of these effects were not found to be significant as seen with NFκB p65 (**Figure 11**).

For STAT1, treatment with LPS was observed to slightly increase phosphorylated STAT1 (pSTAT1) versus the no treatment control baseline, although the effect did not hold statistical significance (1.0 vs 1.3±0.1, P=0.2493, n=13). Pre-treatment with the silent agonist pCF_3 diEPP prior to LPS stimulation appeared to minimally reduce levels of pSTAT1, though this effect was deemed insignificant versus the LPS comparative group (1.3±0.1 vs 1.1±0.1, P=0.1102, n=13). For controls, samples treated with DMSO only and pCF_3 gave resemblance to the no treatment baseline (1.0 vs 0.9±0.06; 0.9±0.06, n=12, respectively). As seen in **Figure 12**, pCF_3 diEPP did not significantly modulate LPS-induced STAT1 phosphorylation.

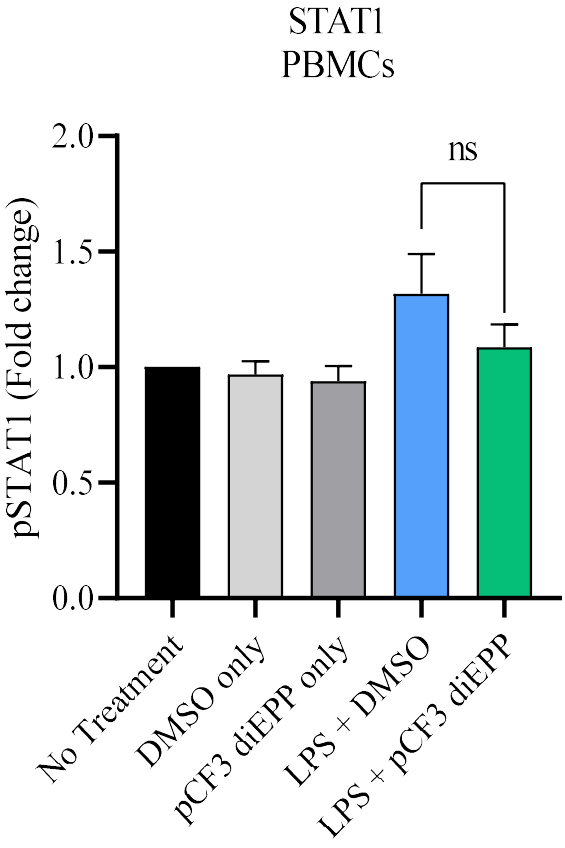

Figure 12: The silent agonist pCF_3 diEPP-modulated phosphorylation of STAT1 in the presence of LPS stimuli Following the collection of human whole blood, peripheral blood mononuclear cells were isolated and separated into 5 different conditions. Respective conditions were stimulated with LPS (100 ng/mL) for 30 minutes, in the presence of 0.1% DMSO or pCF_3 diEPP at a concentration of 100 µM. For controls, PBMC samples were treated with pCF_3 diEPP alone or with 0.1% DMSO alone. The no treatment condition served as a baseline for the fold change of pSTAT1. The α7 nAChR silent agonist pCF_3 diEPP-modulated phosphorylation of STAT1. The cell culture supernatant was analyzed by performing a Bio-Plex Phosphorylation Assay followed by FACS analysis. LPS stimulation prompted a small increase in pSTAT1 levels, while pCF_3 diEPP decreased pSTAT1 levels insignificantly, as observed in the fold change between the LPS + DMSO and LPS + pCF_3 diEPP conditions. Data shown are fold change means ± SEM (n= 13). The letters 'ns' denote non-significant findings between the LPS + pCF_3 diEPP treatment and LPS + DMSO comparative group, using a RM one-way ANOVA, Dunnett's multiple comparisons test.

For STAT3, LPS-treated samples were observed to minimally increase levels of phosphorylated STAT3 (pSTAT3) versus the no treatment control group; however, the effect did not reach statistical significance (1.0 vs 1.2±0.1, P=0.2086, n=13). Pre-treatment with pCF_3 diEPP followed by LPS stimulation weakly modulated levels of pSTAT3, though ultimately the effect was non-significant (1.2±0.1 vs 1.1±0.09, P=0.1985, n=13). For controls, samples treated with DMSO only and pCF_3 diEPP only were found to be similar to the no treatment baseline (1.0 vs 0.98±0.06; 0.9±0.06, respectively). As seen in **Figure 13**, pre-treatment with the silent agonist pCF_3 diEPP did not significantly modulate the LPS-induced phosphorylation of STAT3.

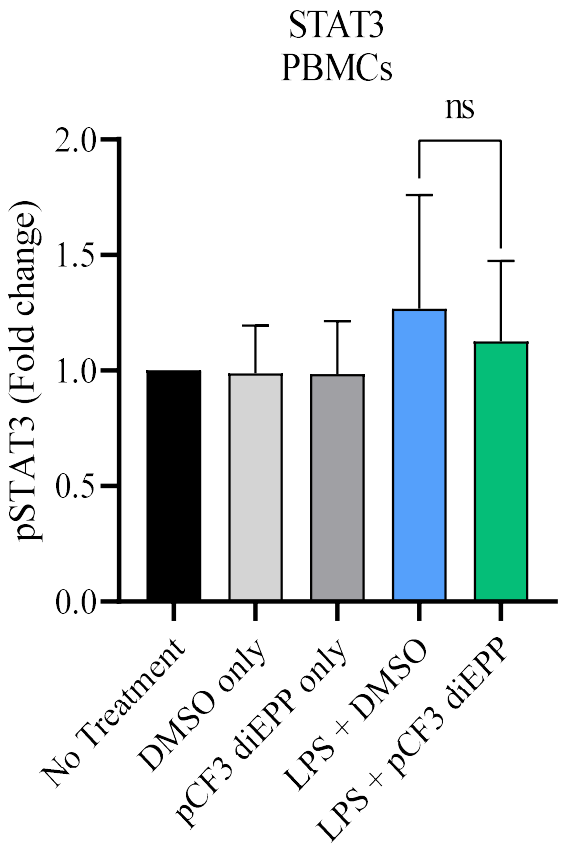

Figure 13: The silent agonist pCF_3 diEPP-modulated phosphorylation of STAT3 in the presence of LPS stimuli Following the collection of human whole blood, peripheral blood mononuclear cells were isolated and separated into 5 different conditions. Respective conditions were stimulated with LPS (100 ng/mL) for 30 minutes, in the

presence of 0.1% DMSO or pCF3 diEPP at a concentration of 100 µM. For controls, PBMC samples were treated with pCF3 diEPP alone or with 0.1% DMSO alone. The no treatment condition served as a baseline for the fold change of pSTAT3. The α7 nAChR silent agonist pCF3 diEPP-modulated phosphorylation of STAT3. The cell culture supernatant was analyzed by performing a Bio-Plex Phosphorylation Assay followed by FACS analysis. LPS stimulation induced a moderate increase in pSTAT3 levels, while pCF3 diEPP decreased pSTAT3 levels insignificantly, observed in the fold change between the LPS + DMSO and LPS + pCF3 diEPP groups. Data shown are fold change means ± SEM (n= 13). The letters 'ns' denote non-significant findings between the LPS + pCF3 diEPP treatment and LPS + DMSO comparative group, using a RM one-way ANOVA, Dunnett's multiple comparisons test.

For AKT, LPS-treated samples were seen to increase the levels of phosphorylated AKT (pAKT) from the no treatment group and was found to be statistically significant (1.0 vs 1.5±0.1, P=0.0358, n=13). Pre-treatment of cells with the silent agonist pCF_3 diEPP was observed to minimally decrease LPS-induced phosphorylation of AKT; however, the effect was non-significant (1.5±0.1 vs 1.3±0.1, P=0.1453, n=13). For the controls, the DMSO only and pCF_3 diEPP only groups (0.9±0.04 and 0.9±0.06, respectively) maintained similar results to the no treatment condition. As seen in **Figure 14**, pre-treatment with pCF_3 diEPP did not significantly modulate LPS-induced phosphorylation of AKT.

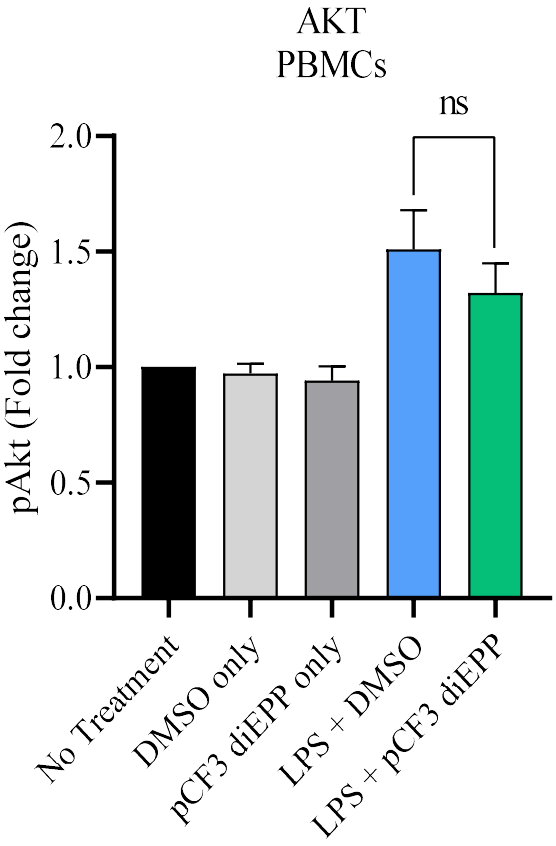

Figure 14: The silent agonist pCF$_3$ diEPP-modulated phosphorylation of AKT in the presence of LPS stimuli Following the collection of human whole blood, peripheral blood mononuclear cells were isolated and separated into 5 different conditions. Respective conditions were stimulated with LPS (100 ng/mL) for 30 minutes, in the presence of 0.1% DMSO or pCF3 diEPP at a concentration of 100 µM. For controls, PBMC samples were treated with pCF3 diEPP alone or with 0.1% DMSO alone. The no treatment condition served as a baseline for the fold change of pAKT. The α7 nAChR silent agonist pCF3 diEPP-modulated phosphorylation of AKT. The cell culture supernatant was analyzed by performing a Bio-Plex Phosphorylation Assay followed by FACS analysis. LPS stimulation induced a moderate increase in pAKT levels, while pCF3 diEPP decreased pAKT levels insignificantly, observed in the fold change between the LPS + DMSO and LPS + pCF3 diEPP groups. Data shown are fold change means ± SEM (n= 13). The letters 'ns' denote non-significant findings between the LPS + pCF3 diEPP treatment and LPS + DMSO comparative group, using a RM one-way ANOVA, Dunnett's multiple comparisons test.

For ERK1/2, phosphorylation of ERK1/2 (pERK1/2) was found to be moderately higher in LPS-treated samples versus the no treatment group, however the effect did not

reach statistical significance (1.0±0.00 vs 1.6±0.21, P=0.0727, n=13). It was observed that pre-treatment with the silent agonist pCF_3 diEPP minimally decreased LPS-induced phosphorylation of ERK1/2; however, the effect was non-significant (1.6±0.21 vs 1.3±0.17, P=0.3922, n=13). For the controls, the DMSO only and pCF_3 diEPP only groups (0.99 ±0.091 and 0.86 ±0.084, respectively) retained comparable outcomes to the no-treatment group. As seen in **Figure 15**, pre-treatment with pCF_3 diEPP did not significantly modulate the LPS-induced phosphorylation of ERK1/2.

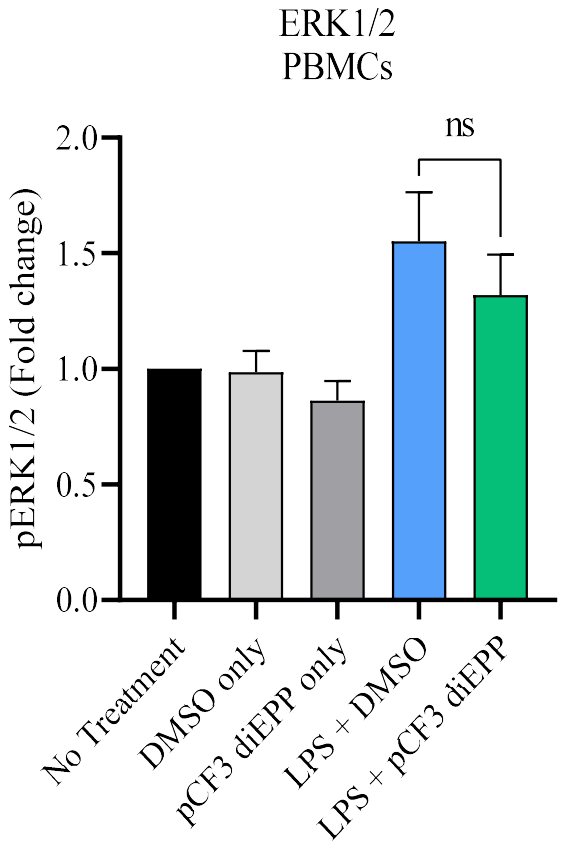

Figure 15: Silent agonist pCF_3 diEPP-modulated phosphorylation of ERK1/2 in the presence of LPS stimuli Following the collection of human whole blood, peripheral blood mononuclear cells were isolated and separated into 5 different conditions. Respective conditions were stimulated with LPS (100 ng/mL) for 30 minutes, in the presence of 0.1% DMSO or pCF_3 diEPP at a concentration of 100 µM. For controls, PBMC samples were treated with pCF_3 diEPP alone or with 0.1% DMSO alone. The no

treatment condition served as a baseline for the fold change of pERK1/2. The α7 nAChR silent agonist pCF_3 diEPP-modulated phosphorylation of ERK1/2. The cell culture supernatant was analyzed by performing a Bio-Plex Phosphorylation Assay followed by FACS analysis. LPS stimulation induced a moderate increase in pERK1/2 levels, while pCF_3 diEPP decreased pERK1/2 levels insignificantly, observed in the fold change between the LPS + DMSO and LPS + pCF_3 diEPP groups. Data shown are fold change means ± SEM (n= 13). The letters 'ns' denote non-significant findings between the LPS + pCF_3 diEPP treatment and LPS + DMSO comparative group, using a RM one-way ANOVA, Dunnett's multiple comparisons test.

4.1.6 Silent agonist pCF3 diEPP modulated LPS-induced phosphorylation of NFκB p65, STAT1, STAT3, Akt, ERK1/2 in Monocytes

When compared to the no treatment control group, LPS-treated samples were found to moderately increase the phosphorylation of NFκB p65 (1.0 vs 1.6±0.3, P=0.2619, n=8), although the effect was not significant. When compared with the LPS+DMSO group, silent agonist treated samples prior to LPS stimulation were found to moderately increase NFκB p65 phosphorylation (1.6±0.3 vs 2.0±0.2, P=0.3932, n=8). Treatments with pCF_3 diEPP alone (0.9±0.1, n=8) or DMSO alone (0.9±0.1, n=8) did not appear to vary from the no-treatment group. Shown in **Figure 16**, LPS-induced NFκB p65 phosphorylation in monocytes increased non-significantly in the presence of the silent agonist pCF_3 diEPP. Note that while statistics were performed, the determined sample size (n) of 11 was not reached, thus conclusions cannot be made.

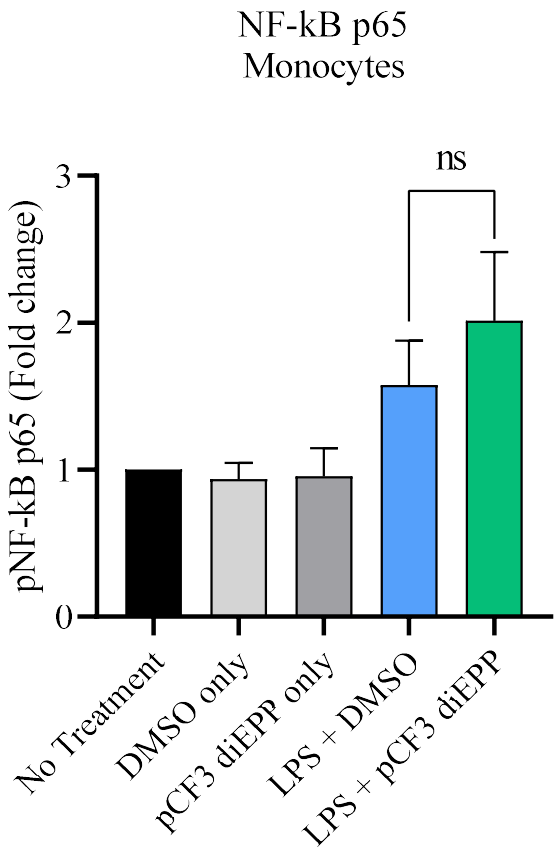

Figure 16: The silent agonist pCF_3 diEPP-modulated phosphorylation of NFκB p65 in the presence of LPS stimuli Following the collection of human whole blood, peripheral blood mononuclear cells were isolated. MACs sorting was further used to collect enriched monocytes. Samples were separated into 5 different conditions. Respective conditions were stimulated with LPS (100 ng/mL) for 30 minutes, in the presence of 0.1% DMSO or pCF_3 diEPP at a concentration of 100 µM. For controls, samples were treated with pCF_3 diEPP alone or with 0.1% DMSO alone. The no treatment condition served as a baseline for the fold change of pNFκB p65. The cell culture supernatant was analyzed by performing a Bio-Plex Phosphorylation Assay followed by FACS analysis. LPS increased pNFκB p65 levels, while pCF_3 diEPP further upregulated pNFκB p65 levels, as observed in the fold change increase between the LPS + DMSO and LPS + pCF_3 diEPP conditions. Data shown are fold change means ± SEM (n=8). The symbol ns denotes non-significant findings between the LPS + pCF_3 diEPP treatment and LPS + DMSO comparative group using a RM one-way ANOVA, Dunnett's multiple comparisons test.

For STAT1, LPS-treated samples led to an observed fold change increase in phosphorylated STAT1 (pSTAT1) from the no treatment control baseline, although the effect did not hold statistical significance (1.0 vs 1.3±0.09, P=0.5190, n=8). pCF_3 diEPP-treated samples prior to LPS stimulation appeared to slightly reduce levels of pSTAT1 versus the LPS+DMSO comparative group, however the effect was deemed insignificant (1.3±0.09 vs 1.1±0.1, P=0.3932, n=8). For controls, samples treated with DMSO only (1.0±0.1, n=8) or pCF_3 diEPP only (0.9±0.1, n=8) did not appear to differ from the no treatment group. Seen in **Figure 17**, pre-treatment with pCF_3 diEPP did not significantly modulate the LPS-induced phosphorylation of STAT1.

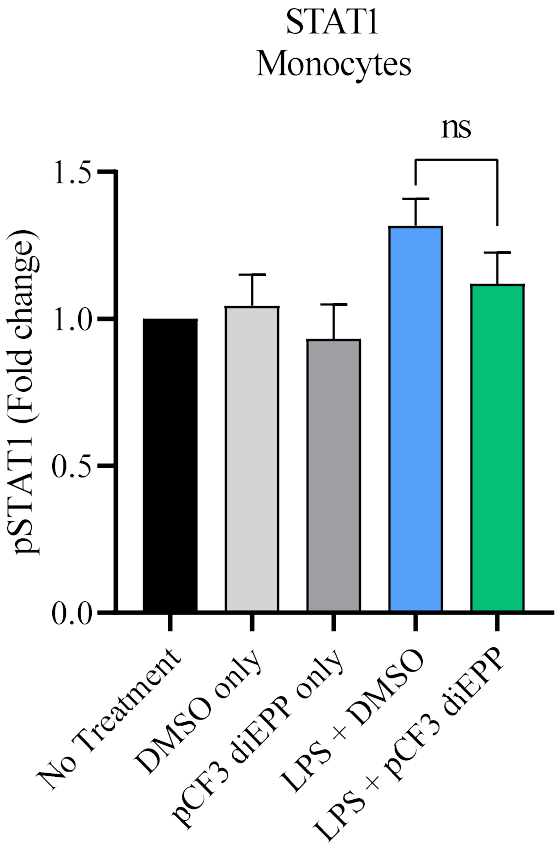

Figure 17: The silent agonist pCF_3 diEPP-modulated phosphorylation of STAT1 in the presence of LPS stimuli Following the collection of human whole blood, peripheral

blood mononuclear cells were isolated. MAC sorting was further used to collect enriched monocytes. Samples were separated into 5 different conditions. Respective conditions were stimulated with LPS (100 ng/mL) for 30 minutes, in the presence of 0.1% DMSO or pCF_3 diEPP at a concentration of 100 µM. For controls, samples were treated with pCF_3 diEPP alone or with 0.1% DMSO alone. The no treatment condition served as a baseline for the fold change of pSTAT1. The cell culture supernatant was analyzed by performing a Bio-Plex Phosphorylation Assay followed by FACS analysis. LPS stimulation prompted a small increase in pSTAT1 levels, while pCF_3 diEPP decreased pSTAT1 levels insignificantly, as observed in the fold change between the LPS + DMSO and LPS + pCF_3 diEPP conditions. Data shown are fold change means ± SEM (n=8). The letters 'ns' denote non-significant findings between the LPS + pCF_3 diEPP treatment and LPS + DMSO comparative group, using a RM one-way ANOVA, Dunnett's multiple comparisons test.

For STAT3, LPS stimulation was observed to slightly increase phosphorylated STAT3 (pSTAT3) versus the no treatment control group; however, the effect did not reach statistical significance (1.0 vs 1.2±0.1, P=0.1021, n=8). pCF_3 diEPP-treated samples prior to LPS stimulation appeared to experience minimal reduced levels of pSTAT3, however the effect was non-significant (1.2±0.1 vs 1.1±0.1, P=0.4770, n=8). For controls, samples treated with DMSO only (1.1±0.05, n=8) or pCF_3 diEPP only (0.8±0.2, n=8) were observed to compare to the no treatment baseline. Seen in **Figure 18**, pre-treatment with pCF_3 diEPP did not significantly modulate the LPS-induced phosphorylation of STAT3.

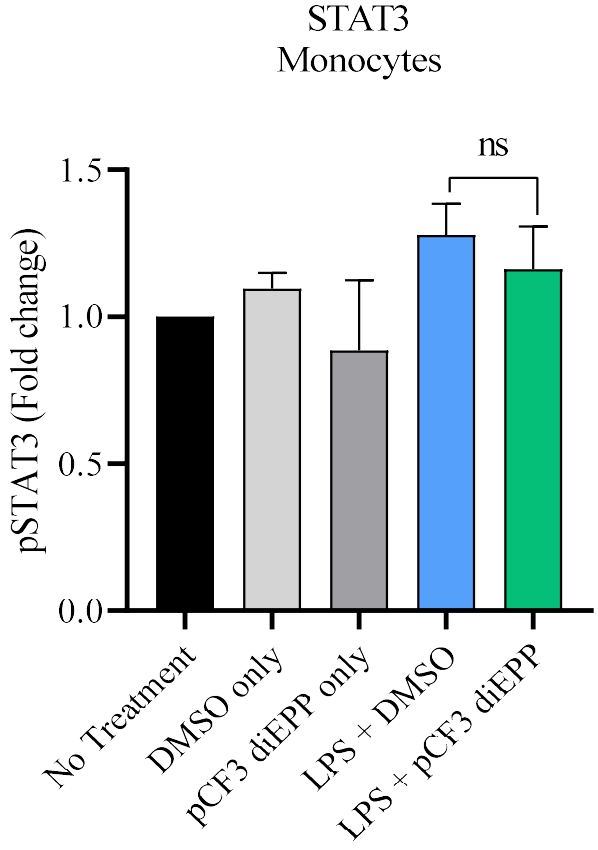

Figure 18: The silent agonist pCF_3 diEPP-modulated phosphorylation of STAT3 in the presence of LPS stimuli Following the collection of human whole blood, peripheral blood mononuclear cells were isolated. MAC sorting was further used to collect enriched monocytes. Samples were separated into 5 different conditions. Respective conditions were stimulated with LPS (100 ng/mL) for 30 minutes, in the presence of 0.1% DMSO or pCF_3 diEPP at a concentration of 100 µM. For controls, samples were treated with pCF_3 diEPP alone or with 0.1% DMSO alone. The no treatment condition served as a baseline for the fold change of pSTAT3. The cell culture supernatant was analyzed by performing a Bio-Plex Phosphorylation Assay followed by FACS analysis. LPS stimulation induced a moderate increase in pSTAT3 levels, while pCF_3 diEPP decreased pSTAT3 levels insignificantly, observed in the fold change between the LPS + DMSO and LPS + pCF_3 diEPP groups. Data shown are fold change means ± SEM (n=8). The letters 'ns' denote non-significant findings between the LPS + pCF_3 diEPP treatment and LPS + DMSO comparative group, using a RM one-way ANOVA, Dunnett's multiple comparisons test.

The phosphorylation of AKT (pAKT) was observed to moderately increase in LPS-treated samples when compared to the no treatment group, however the effect did not reach statistical significance (1.0 vs 1.6±0.1, P=0.1417, n=8). Pre-treatment with the silent agonist pCF_3 diEPP seemed to minimally reduce LPS-induced phosphorylation of AKT (1.6±0.1 vs 1.5±0.2, P=0.7114, n=8) although the effect was non-significant. For the controls, the DMSO only and pCF_3 diEPP only groups (1.0±0.09 and 1.0±0.2, respectively) maintained similar results to the no treatment condition. Shown in **Figure 19**, pre-treatment with pCF_3 diEPP did not significantly modulate the LPS-induced phosphorylation of AKT.

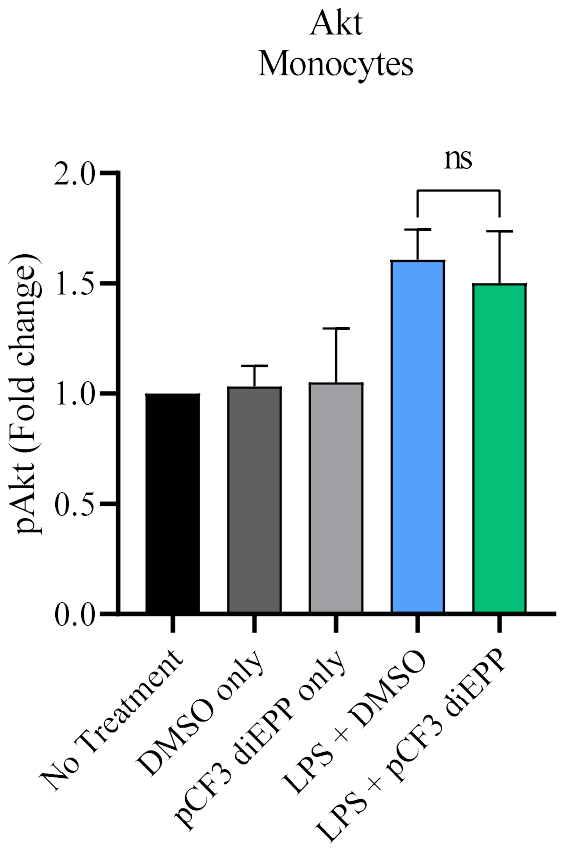

Figure 19: The silent agonist pCF_3 diEPP-modulated phosphorylation of AKT in the presence of LPS stimuli Following the collection of human whole blood, peripheral

blood mononuclear cells were isolated. MAC sorting was used to collect enriched monocytes. Samples were separated into 5 different conditions. Respective conditions were stimulated with LPS (100 ng/mL) for 30 minutes, in the presence of 0.1% DMSO or pCF_3 diEPP at a concentration of 100 µM. For controls, samples were treated with pCF_3 diEPP alone or with 0.1% DMSO alone. The no treatment condition served as a baseline for the fold change of pAKT. The cell culture supernatant was analyzed by performing a Bio-Plex Phosphorylation Assay followed by FACS analysis. LPS stimulation induced a moderate increase in pAKT levels, while pCF_3 diEPP decreased pAKT levels minutely, as observed in the fold change between the LPS + DMSO and LPS + pCF_3 diEPP groups. Data shown are fold change means ± SEM (n= 8). The letters 'ns' denote non-significant findings between the LPS + pCF_3 diEPP treatment and LPS + DMSO comparative group, using a RM one-way ANOVA, Dunnett's multiple comparisons test.

For ERK1/2, LPS-treated samples were observed to slightly increase the level of phosphorylated ERK1/2 (pERK1/2) versus the no treatment group, however the effect did not reach statistical significance (1.0 vs 1.3±0.1, P=0.0756, n=8). Pre-treatment with the silent agonist pCF_3 diEPP was seen to have a modest reduction in LPS-induced ERK1/2 phosphorylation; however, the effect was non-significant (1.3±0.1 vs 1.0±0.1, P=0.1024, n=8). For the controls, the DMSO only or pCF_3 diEPP only groups (1.0±0.09 and 0.9±0.1, n=8, respectively) appeared to have comparable outcomes versus the no-treatment group. As seen in **Figure 20**, pre-treatment with pCF_3 diEPP did not significantly modulate LPS-induced phosphorylation of ERK1/2.

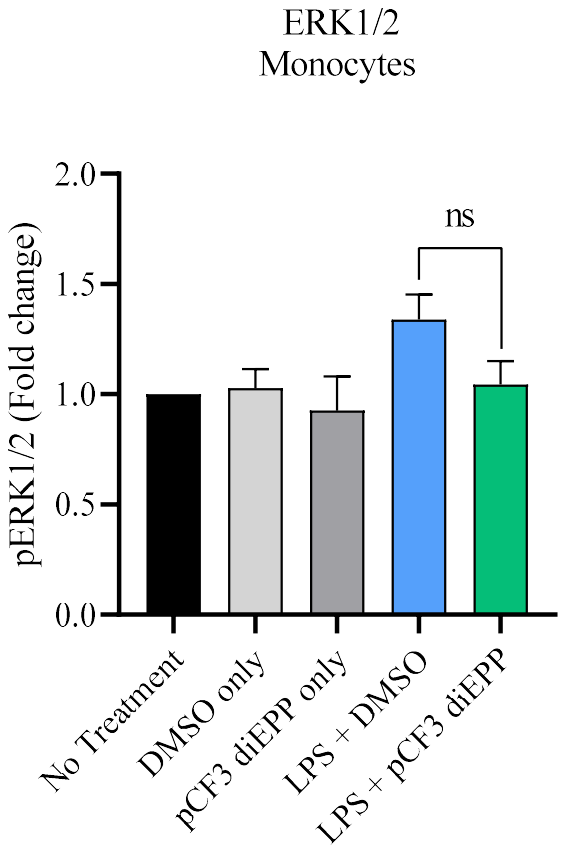

Figure 20: Silent agonist pCF_3 diEPP-modulated phosphorylation of ERK1/2 in the presence of LPS stimuli Following the collection of human whole blood, peripheral blood mononuclear cells were isolated. MAC sorting was further used to collect enriched monocytes. Samples were separated into 5 different conditions. Respective conditions were stimulated with LPS (100 ng/mL) for 30 minutes, in the presence of 0.1% DMSO or pCF_3 diEPP at a concentration of 100 µM. For controls, samples were treated with pCF_3 diEPP alone or with 0.1% DMSO alone. The no treatment condition served as a baseline for the fold change of pERK1/2. The cell culture supernatant was analyzed by performing a Bio-Plex Phosphorylation Assay followed by FACS analysis. LPS stimulation induced a moderate increase in pERK1/2 levels, while pCF_3 diEPP decreased pERK1/2 levels, observed in the fold change between the LPS + DMSO and LPS + pCF_3 diEPP groups. Data shown are fold change means ± SEM (n=8). The letters 'ns' denote non-significant findings between the LPS + pCF_3 diEPP treatment and LPS + DMSO comparative group, using a RM one-way ANOVA, Dunnett's multiple comparisons test.

4.1.6 Silent agonist m-bromo-PEP modulation of M1/M2 cell phenotyping in PBMCs

This experiment assessed the markers CD14, CD16, CD11c, CD36, CCR2, and HLA-DR to study how the silent agonist m-bromo-PEP modulated M1/M2 cell phenotyping in human PBMCs. Silent agonist pre-treatment of samples did not appear to modulate LPS-induced marker expression versus the non-stimulated group: CD14 (4.4±1.2 vs 2.6±0.6, P=0.1709, n=18, respectively), CD16 (12.9±1.3 vs 10.6±1.1, P=0.0488, n=18, respectively), CD36 (7.1±1.4 vs 5.7±0.7, P=0.4012, n=18, respectively), CCR2 (3.6±1.0 vs 1.3±0.2, P=0.0733, n=18, respectively), CD11c (4.4±1.1 vs 2.3±0.4, P=0.1196, n=18, respectively), and HLA-DR (9.7±1.4 vs 8.2±0.8, P=0.2431, n=18, respectively). As seen in **Figure 21**, comparison between the NO LPS+DMSO group versus the LPS+DMSO group shows an LPS-induced decrease of all markers studied, although the effects are mostly insignificant.

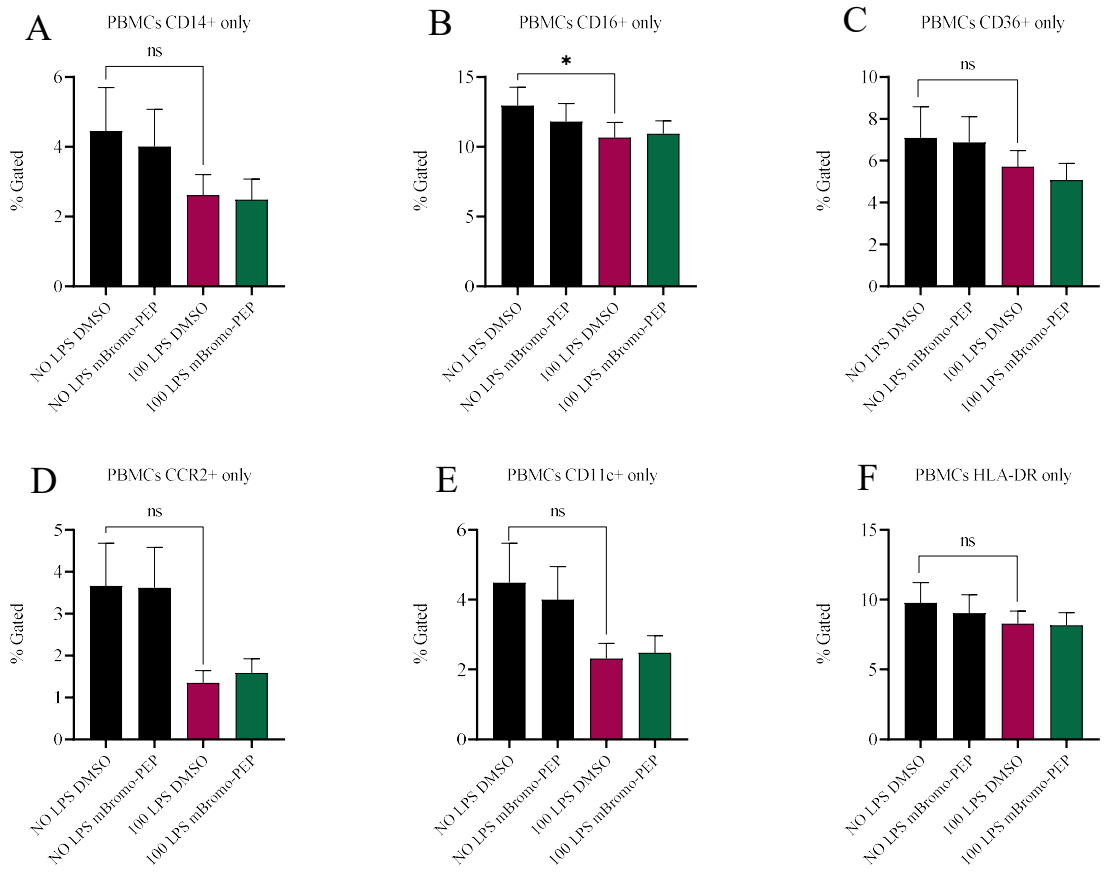

Figure 21: Cell surface marker expression in PBMCs Following the collection of human whole blood from healthy volunteers, PBMCs were isolated and cultured in 6-well plates. Cells were stimulated with LPS (100ng/mL) for 48 hours and then stained with antibodies for surface markers CD14, CD16, CD36, CD11c, CCR2, and HLA-DR. Treatment with LPS appeared to moderately decrease the expression of markers in Figures 18A, 18C, and 18E, but did so weakly in Figures 18B, 18D, and 18F. Data shown are means ± SEM (n=18). The letters 'ns' denotes non-significant findings, while the symbol * denotes statistically significant findings between the NO LPS + DMSO treatment and the LPS + DMSO comparative group (*: $P \leq 0.05$; **: $P \leq 0.01$, ***: $P \leq 0.001$) using a RM one-way ANOVA, Dunnett's multiple comparisons test.

5.0 Discussion

Recent evidence that molecules such as nicotine can reduce pro-inflammatory responses by desensitizing non-neuronal α7 nAChRs has led to the design of unique pharmacological molecules known as silent agonists[91]. Patch clamp experiments reveal that the ion channel activity of α7 nAChRs (defined as the translocation of ions across the membrane) are suggested to be absent in PBMCs[93,94]. These observations are critical, for they suggest that the principle signaling events by which non-neuronal nAChRs modulate inflammation occur through means other than ion exchange mechanisms. Studies have shown that dose-dependent concentrations of nicotine (0.1-100 μM) have anti-inflammatory effects and readily desensitize nAChRs at concentrations above 1μM[67]. To put that in perspective, a study by Gourley *et al.* demonstrated that nicotine concentrations in the arterial blood, following cigarette smoking, ranged between 20-60ng/mL[95]. Common nAChR agonists such as nicotine and acetylcholine can target multiple nAChR subtypes and are therefore vulnerable to off-target binding effects. For such reasons, the ability for silent agonists to produce minimal to no channel opening by selectively promoting and prolonging the desensitized state made the study of these molecules desirable[73].

Silent agonists targeting α7 nAChRs have been shown to delay disease progression and decrease severity in animal models of inflammation[91]. The capacity for these molecules to elicit a physiological response despite their inability to open channels on their own gives credence to proposed metabotropic signaling pathways for α7 receptors[96]. However, the precise nature of said mechanisms remain the epicenter of much debate. Most works relating to silent agonists have been performed in murine

models; thus, the extent by which α7 nAChR silent agonists can modulate the immune response in human blood immune cells is unknown. Hence, this study set out to investigate the hypothesis that α7 nAChR silent agonists modulate LPS-induced cytokine secretion, pro-inflammatory signaling pathways, and cell phenotyping in these cells.

The current data indicates that 1hr pre-treatments with the silent agonist pCF_3 diEPP significantly decreased LPS-induced secretion of pro-inflammatory cytokines IL-1β, IL-6, and TNF-α, but did not alter the levels of the anti-inflammatory cytokine IL-10 in human whole blood. Other silent agonists used in the study did not perform akin to pCF_3 diEPP, at times failing to modulate LPS-induced cytokine secretion altogether or having small effects at best. 24hr pre-treatments with the silent agonists prior to LPS stimulation failed to modulate cytokine secretion significantly. While it may imply a lack of drug efficacy at this time point, it is possible that other factors independent of nAChR activity such as cell stress, death and/or decrease in receptor turnover took place. Such events can induce cytokine secretion and impair interpretation of findings.

Cell signaling studies revealed that pre-treatment with the silent agonist pCF_3 diEPP significantly decreased LPS-induced NFκB p65 phosphorylation, but did not significantly modulate the phosphorylation of STAT1, STAT3, AKT, and ERK1/2 in PBMCs. Although the effect was non-significant, trends observed showed these phosphoproteins experienced a moderate decrease in their phosphorylation. In our monocyte signaling studies, we found that the silent agonist pCF_3 diEPP modulated the phosphoproteins STAT1, STAT3, AKT, and ERK1/2 in a similar fashion as the PBMCs. In contrast, our silent agonist strongly upregulated the phosphorylation of NFκB p65.

Due to unforeseen circumstances, the desired sample size (n=11) was not achieved, thus statistical conclusions could not be made.

Finally, in our cell phenotype studies, we set out to study the markers CD14, CD16, CD36, CCR2, HLA-DR, and CD11c in order to understand how our silent agonists modulate phenotypes pertaining to M1/M2 monocytes and other immune cells of interest. Despite efforts, we failed to see any effect with LPS stimulation from our PBMC culture, thus making it difficult to determine the extent by which our silent agonists could play a role in this study.

5.1.0 Effects of silent agonists on LPS-induced cytokine secretion

As expected, the α7 nAChR selective silent agonist pCF_3 diEPP was shown to significantly decrease levels of LPS-induced pro-inflammatory cytokines IL-1β, IL-6, and TNF-α, while not affecting levels of anti-inflammatory cytokine IL-10 in whole blood. Another pro-inflammatory cytokine, IL-12, was studied in pilot experiments; however, since we could not measure detectable levels of this cytokine (data not shown), further study was subsequently dropped. Monocytes in the periphery account for the majority of cytokine release; thus when exposed to inflammatory stimuli such as LPS, they secrete a diverse portfolio of pro-inflammatory cytokines[97]. Not surprising then, activation of α7 nAChRs on monocytes and macrophages are primarily responsible for the inhibition of pro-inflammatory cytokines[64]. A study by Hamano *et al.,* 2006, found that in monocytes isolated from the blood of healthy human donors, stimulation of α7 nAChRs with nicotine significantly reduced levels of TNF-α but did not alter IL-10 secretion[98]. Thus, our present data are in line with these findings and further support a

role for nAChR-related agonists in suppressing the secretion of pro-inflammatory cytokines.

In another study, the α7 nAChR partial agonist GTS-21, significantly inhibited the secretion of IL-6 and TNF-α in *ex vivo* cultures of LPS-induced primary mouse macrophages endogenously expressing α7 nAChRs[99]. Furthermore, a study by Liu *et al.,* using the drug PNU-282987, a potent and selective agonist for neuronal α7 nAChRs, was able to significantly decrease IL-1β and TNF-α expression levels[100]. These effects were blocked with the administration of α-bungarotoxin, a known competitive antagonist of nAChRs[100]. Finally, recent work by Godin *et al.*, in 2020, showed that the silent agonist m-bromo PEP was able to reduce pro-inflammatory mouse bone marrow-derived monocyte/macrophage (BMDM) numbers, cytokine production, and significantly improved disease outcome in EAE mice[91]. These results, along with our findings, reinforce the hypothesis that cytokine secretion can be modulated via the desensitizing ability of nAChRs.

Other silent agonists used in this study were m-bromo PEP, $mCONH_2$ diEPP bromide, and $mCONH_2$ diEPP iodide. As previous studies showed that m-bromo PEP could modulate immune responses in EAE mice[91], we expected similar results in LPS-induced human blood immune cells. However, our study showed that m-bromo PEP failed to modulate levels of any of the pro-inflammatory cytokines studied, implying a lack of efficacy in human cells. We saw that the silent agonist $mCONH_2$ diEPP bromide moderately inhibited the secretion of TNF-α and IL-1β and did not alter IL-10 levels. However, $mCONH_2$ diEPP bromide failed to inhibit IL-6 secretion levels. In contrast,

$mCONH_2$ diEPP iodide was found to inhibit levels of TNF-α and IL-10, but failed to modulate levels of IL-6 and IL-1β.

It is unclear why certain α7 nAChRs silent agonists work in modulating LPS-induced cytokine secretion differently in mice and vice versa in humans, however, studies have suggested that the natural genetic variabilities of nAChRs that exist between humans and mice influence molecule sensitivity to nAChRs, nAChR expression, pharmacokinetics, functionality and structure[101]. Thus, it is possible that structural differences between silent agonists can limit the extent by which they can act on nAChRs and modulate cytokine secretion. Further work will be required to investigate this.

Altogether, the results here further support previous studies demonstrating that α7 nAChRs agonists and silent agonists can counteract the release of pro-inflammatory cytokines without affecting levels of anti-inflammatory cytokines. Since a large majority of autoimmune and inflammatory diseases are characterized by an imbalance of cytokines that often favors pro-inflammatory types[31], we showed that pCF_3 diEPP can promote a homeostatic cytokine milieu.

5.1.1 Effects of silent agonists on LPS-induced phosphorylation of NFκB p65 in PBMCs

As hypothesized, the silent agonist pCF_3 diEPP significantly reduced LPS-induced levels of NFκB p65 phosphorylation in PBMCs (80% inhibition of LPS effect). Our findings support that the anti-inflammatory action of α7 nAChRs in non-neuronal cells is primarily in part of their ability to inhibit NFκB signaling events, thus preventing the transcription of pro-inflammatory genes[102]. For instance, activation of α7 nAChRs in

immunodeficient BALB/c mice with galantamine was shown to ameliorate zymosan-induced acute kidney injury via suppression of the NF-κB p65-high mobility group box protein (HMGB)-1 cycle[103]. HMGB-1 acts as a downstream molecule of NF-κB p65, where it mediates cytokine release and tissue damage by binding toll like receptors.[103] The effects of α7 nAChRs in this study were subsequently reversed by the antagonist methyllycaconitine[103]. Another study showed that α7 nAChR activation provided protection in monosodium iodoacetate-induced osteoarthritis rat models by inhibiting the phosphorylation of NF-κB p65 in chondrocytes[104].

Despite our findings and those previously discussed, the precise mechanisms by which α7 nAChRs inhibit the NF-κB pathway and its activity remain unclear. Since our study only set out to determine whether silent agonists could modulate pro-inflammatory pathways of interest, addressing the specific mechanisms was beyond the scope of this project. That said, recently proposed mechanisms will be discussed to consider the possible ways by which silent agonists inhibited the phosphorylation of NF-κB p65.

One proposed model of study suggests that α7 nAChR activation impedes the phosphorylation of inhibitor of NF-κB (Iκ-B). Under normal conditions, the cellular protein Iκ-B functions to retain NF-κB proteins in the cytoplasm, however, canonical signaling from the activation of cytokine surface receptors or toll-like receptors prompt the activation of Iκ-B kinase to phosphorylate Iκ-B[64]. Once phosphorylated, Iκ-B is degraded by a proteasome, and NF-κB translocates to the nucleus[64]. In 2006, Yoshikawa *et al.,* proposed a mechanism suggesting that agonist binding to α7 nAChRs could inhibit the phosphorylation of Iκ-B, thus retaining NF-κB in the cytoplasm and suppressing its function[105].

Collectively, the numerous mechanisms outlined here demonstrate the vast complexity involved in α7 nAChR mediated NF-κB signaling. It is possible that the downregulation of NF-κB p65 induced by silent agonists could utilize any one of these mechanisms. Our findings did not show statistically significant modulation of STAT1/STAT3 phosphorylation in either human PBMC or monocyte cultures, which suggests that the anti-inflammatory mechanism(s) activated following silent agonist binding to α7 nAChRs are not related to the JAK/STAT pathway. Further work will be needed to determine if this is the case.

5.1.2 Effects of silent agonists on LPS-induced phosphorylation of NF-κB in monocytes

It is important to note that this study did not reach full completion. A sample size n of 11 was to be acquired, however recent events pertaining to the COVID-19 pandemic stopped further sample acquisition, ending with a sample size n of 8. Thus, statistical conclusions regarding this study aim could not be made. Interpretation of current results may not accurately reflect the outcome and are subject to change. Our study found that the α7 nAChR silent agonist pCF_3 diEPP did not follow the hypothesized trend that silent agonists decrease LPS-induced phosphorylation of NF-κB p65 (pNF-κB p65) in monocytes.

Instead, silent agonist treatment prior to LPS stimulation resulted in increased levels of pNF-κB p65 (44% increase from the LPS effect). While such findings contradict aspects of the literature[64,87], recent knowledge pertaining to the biology of monocytes indicate that the observed effect by silent agonist treatment may be anti-inflammatory. As

monocytes critically require NF-κB for their differentiation and survival, they accumulate large NF-κB reservoirs in their cytoplasm to effectively ensure a rapid NF-κB response upon activation by stimuli[106]. Myeloid cell-specific deletions of the central NF-κB activator IKKβ in mice were shown to influence the polarization of these cells toward the inflammatory M1 subset[106]. These results suggest that in monocytes, IKKβ and NF-κB have roles for polarization towards the anti-inflammatory M2 subset, thus promoting tissue repair and attenuating inflammation[107].

Following this point, a study using transgenic mice with myeloid-specific upregulation of NF-κB p65 resulted in reduced lesion formation and foam cell production in a model of atherosclerosis, a disease largely governed by the infiltration of M1 monocytes[108]. Moreover, *Cre*/*lox*-mediated gene targeting of IKKβ in lung epithelial cells showed that IKKβ deletion inhibited inflammation and prevented clearance of bacteria in the lung; however, IKKβ-specific deletion in macrophages increased the inflammatory response in this model of study[107]. In addition, the same study provided evidence that IKKβ activation inhibited M1 macrophage phenotype and negatively regulated STAT1[107]. In the context of inflammation, these findings indicate a protective role for NF-κB in myeloid cells through IKKβ activation. Future studies should investigate how silent agonists modulate the phosphorylation of IKKβ in myeloid-specific studies to complement the findings observed regarding NF-κB.

Finally, a recent study in 2016 by Schwabe *et al.,* provides further evidence to suggest that pCF_3 diEPP upregulation of pNF-κB p65 is anti-inflammatory. As the phosphorylation of NF-κB p65 at the IKK phosphorylation site S536 is believed to be crucial for NF-κB translocation to the nucleus in humans, Schwabe *et al.,* conducted

experiments using knock-in mice S534A with mutant p65 alanine-to-serine substitution at position 534 (a confirmed mouse homolog of human S536) and observed that following LPS stimulation, S534A mice experienced increased mortality in comparison to WT mice[109]. These studies further suggest that S534 phosphorylation in mice may not be required for nuclear translocation; rather, it suppresses NF-κB signaling to ultimately prevent inflammation[109]. The authors suggest that S534/S536 phosphorylation of NF-κB p65 negatively regulates its stability and the NF-κB pathway altogether[109]. Thus, it is possible that since silent agonists acting through α7 nAChRs appear to upregulate pNF-κB p65 levels, they subsequently promote negative-feedback mechanisms that function to counteract the pro-inflammatory actions of NF-κB. Since S536 phosphorylation of NF-κB p65 has been shown to negatively regulate NF-κB-dependent genes (e.g tnf & IkB), our experiments could use microarray techniques to comparatively measure the expression of such genes between LPS-treated samples and samples pre-treated with silent agonists prior to stimulation. Because silent agonist treated samples appear to increase S536 site phosphorylation of NF-κB p65, we would expect to see reduced expression of NF-κB-dependent genes that subsequently promote anti-inflammatory effects.

To further confirm our observations that silent agonists upregulated phosphorylation of NF-κB p65 in monocyte-specific samples, we could perform a western blot analysis using phospho-specific antibodies, ELISA techniques, or mass spectrometry. Moreover, it may be beneficial to use cytometric bead array applications to quantify the levels of cytokines in LPS-treated monocyte-specific samples versus samples

pre-treated with silent agonists to elucidate if our observations have anti-inflammatory effects.

5.1.3 Effects of silent agonists on LPS-induced phosphorylation of STAT1, STAT3, Akt, and ERK1/2

In this study, the silent agonist pCF_3 diEPP was found to modulate the LPS-induced phosphorylation of phosphoproteins. Although these effects were not statistically significant, we did observe some considerable trends. To briefly summarize, we found that for STAT1, STAT3, Akt, and ERK1/2, protein phosphorylation decreased by 20%, 10%, 20%, and 30% in PBMCs respectively; while for monocytes, protein phosphorylation decreased by 20%, 12%, 11%, and 29%, respectively. It is possible that we did not have sufficient statistical power to capture an effect; thus, a larger sample size may be required.

Considering that cholinergic agonists such as acetylcholine have been shown to modulate the dysfunction of all inflammatory pathways studied here[110,111], our findings are unexpected. In retrospect, there are several factors that could have affected our results. For this study, a 30-minute LPS stimulation time point was considered optimal, given that a similar study previously conducted in our lab had observed a measurable increase in activation of the various pathways. Despite this, it is possible that our stimulation time points did not vary sufficiently to accurately capture LPS-induced responses in these pathways.

To explore this hypothesis, western blot analysis of rat primary microglial cultures by Kaminska *et al.* showed that phosphorylation levels of STAT1 and STAT3

rapidly increased and reached maximum induction between 1 and 1.5h[112]. For MAPK pathways, conditioned medium from LPS-stimulated PBMCs activated MAPK signaling for a 10 minute period in primary cultures of trophoblasts[113]. In addition, western blot experiments in RAW264.7 macrophage cell line found that LPS induced phosphorylation of ERK1/2 in both the cytoplasm and nucleus reached peak levels between 60-120 minutes[114]. Studies investigating PI3K/Akt signaling events in Jurkat cells and THP-1 human monocytic cell lines were able to show that LPS increased levels of phosphorylated Akt, reaching a peak at 60 minutes[115,116]. For the NF-κB pathway, studies working with the RAW 264.7 macrophage cell line determined that NF-κB nuclear translocation peaked at 30 minutes following LPS stimulation[117]. Apart from NF-κB, these studies suggest that the phosphorylation and subsequent modulation of phosphoproteins by silent agonists was unfeasible with the current LPS stimulation time point of 30 minutes. Thus, future signaling studies will need to further optimize stimulation time points to establish ideal phosphorylation events in our pathways of interest.

To further investigate why the silent agonist pCF_3 diEPP failed to significantly modulate the LPS-induced phosphorylation, it is necessary to discuss the role of stimuli that are needed to activate intracellular signaling pathways. Indeed, the activation of inflammatory pathways involve numerous common mediators that range from microbial products, cytokines, growth factors, osmotic stress, and heat shock[4]. Starting with STAT1 and STAT3, studies suggest that their phosphorylation is triggered primarily through IFN-γ and NF-κB dependent IL-6[117,118]. Recent observations by Bluyssen *et al.,* showed that pre-treatment of endothelial cells with IFN-γ prior to LPS stimulation resulted in a

significant increase of STAT1 protein production and subsequent phosphorylation than individual factors alone[119]. Furthermore, western blot analyses of LPS-induced murine spleen and liver lysates revealed that IL-6 trans signaling (via gp130) strongly enhanced STAT3 phosphorylation, revealing an essential role for IL-6 in facilitating STAT3 phosphorylation in the presence of LPS[120]. Thus, to investigate silent agonist modulation of STAT-dependent pathways, future treatment strategies should incorporate IFN-γ and IL-6 alongside LPS.

For the PI3K/Akt pathway, the phosphorylation of PI3K and subsequent activation of downstream Akt is regulated primarily by growth factors (i.e epidermal and transforming growth factors), cytokine receptors, G-protein coupled receptors, and integrin signaling[121]. For the MAPK pathway, rapid phosphorylation of ERK1/2 is induced by hormones and growth factors such as platelet-derived growth factor and fibroblast growth factor-2[122]. To investigate how silent agonists can modulate these pathways, it would be beneficial to consider the use of such diverse stimulants in addition to LPS. Finally, the observation that LPS significantly upregulated the phosphorylation of NF-κB p65 in our PBMC studies and strongly in monocytes was expected. NF-κB signaling is activated primarily via two TLR adaptors, MyD88 and TRIF[24]. Being a classic Toll-like receptor 4 ligand (TLR4), LPS was the ideal choice and thus provides a reason as to why pCF_3 diEPP only significantly reduced levels of NFκB p65 phosphorylation, following LPS stimulation of PBMCs. Altogether then, our findings with PBMCs and monocytes suggest that LPS alone is not entirely enough to activate JAK/STAT, MAPK, and PI3K/Akt pathways within an inflammatory context.

Finally, while it was observed that the phosphorylation levels of proteins in the JAK/STAT, MAPK, and PI3K/Akt pathways did not experience a statistically significant reduction in both PBMCs and monocytes, a general trend showing a moderate decrease was seen. As the previously discussed JAK/STAT pathway[64] suggests that cholinergic agonists acting on α7 nAChRs upregulate pSTAT3 and suppresses NF-κB transcription activity, the trends seen in this study do not support this model. Rather, current trends appear to suggest that silent agonists act via the unphosphorylated STAT3 (uSTAT3) pathway model, which briefly proposes that uSTAT3 can bind NF-κB in the cytoplasm and prevent its nuclear translocation[107]. Future studies can confirm these observations by measuring total protein fractions (via western blotting or total protein beads) and determining the relative unphosphorylated fraction of the protein of interest.

For the MAPK pathway, the trends seen in this study support those by Zang *et al.,* showing that in the RAW264.7 macrophage cell line, LPS stimulation increased phosphorylation of ERK1/2, but was subsequently inhibited with acetylcholine treatment[123]. As previously mentioned, one study suggested that α7 nAChR agonist-triggered intracellular Ca2+ transients in PC12 cells, thus leading to the activation of calmodulin-dependent protein kinase II and prompting phosphorylation of p38 MAPK, MEK1/2, and ERK1/2[69]. In the presence of α7 nAChR antagonists or chelation of extracellular Ca2+, the effect of α7 nAChR agonism was attenuated, suggesting that MAPK related pathways are mediated mostly by the ionotropic functions of the nAChRs[69]. Thus, it is plausible that the weak decreasing trend seen following pre-treatment with silent agonists was a consequence of silent agonists promoting minimal channel opening. Finally, studies using the RAW264.7 macrophage cell line were able to

show that the α7 nAChR partial agonist GTS-21 suppressed the LPS-induced phosphorylation of Akt, which support the trends seen by silent agonist treatment[87].

Regarding cell signaling findings, the presented results measured phosphorylation for each protein of interest and were normalized with beta-actin. That said, total protein levels were not addressed. This is because we initially sought to determine which pro-inflammatory pathways could be modulated by silent agonists before taking this measure. Due to lab closures in response to COVID-19, we were unable to address total protein levels; however, this shall be completed when the time permits. Indeed, quantifying total protein levels would have allowed us to determine the ratio between phosphorylated and unphosphorylated proteins (total protein). Future studies will need to use Bio-Plex Pro total protein beads to accomplish this task.

5.1.4 Effects of silent agonists on LPS-induced M1/M2 phenotype

Based on flow cytometric analysis, this study revealed that a 48hr LPS stimulation of PBMC cultures was not enough to capture an LPS-induced effect in some markers. This was based on observations that in LPS stimulated samples, cell surface marker expressions for CD14, CD16, CD36, and HLA-DR were not statistically different from control conditions with no treatment. On the contrary, CD11c and CCR2 showed an LPS-induced decreasing trend; however, the effect was non-significant. Given that we did not see any effects from markers that are known to be upregulated by LPS, it is plausible that our observations stem not from LPS-induced biological effects; rather, from external factors that remain to be investigated and optimized. Furthermore,

comparisons between the LPS positive control and samples pre-treated with silent agonists prior to stimulation suggest that silent agonists did not appear to modulate marker expression. Given the doubt of an LPS effect however, this is only speculative.

A study by Obrecht *et al.,* showed that LPS induction strongly enhanced CD14 and CD16 in 45hr cultures of purified human monocytes, while findings by Lin *et al.,* demonstrated that LPS upregulated hepatic CD14 expression in bile duct ligation rats[124,125]. For CD36, a 2017 study by Katoh *et al.,* showed that LPS stimulation enhanced the expression of CD36 in bone marrow macrophages[126]. Regarding chemokine receptor CCR2, a 2006 study by Serbina and Pamer showed that when mice were exposed to LPS, $Ly6C^{hi}$ monocytes depended on CCR2 to migrate from the bone marrow to the circulation[127]. Moreover, a 2014 study by Petit-Paitel *et al.*, found that in the brains of mice injected with LPS (systemic), there was a percent increase of inflammatory monocytes and microglia expressing CCR2, suggesting the recruitment of such cells under inflammatory conditions[128].

CD11c expression is reduced in mouse bone marrow-derived DC (BMDC) upon activation by TLR3/4/9 ligands[129]. Finally, a study by Huang *et al.,* working with THP-1 cells reported that LPS stimulation significantly upregulated HLA-DR; an effect that was dampened by applying norepinephrine[130]. Thus, as supported by findings in the literature, LPS stimulation of PBMCs in this study should have upregulated the expression of CD14, CD16, CD36, and HLA-DR.

One possible explanation for this could be a result of the culture conditions used in this study, which potentially failed to capture LPS induced inflammatory responses.

Recently, Harris *et al.,* optimized a protocol to study human macrophages using PBMC-derived monocytes. Monocytes were pre-differentiated into macrophages by a 6-day culture with M-CSF or GM-CSF[131]. To stimulate M1 and M2 macrophage polarization, they treated monocytes with LPS/IFNγ and IL-4/IL-10/ IL-13/TGF-β, respectively for 24hrs[131]. Similarly, a 2017 study by Karabina *et al.,* obtained monocyte-derived macrophages after 7 days of culture in complete medium. Cells were polarized towards M1 or M2 cells via 24hr treatments of 100ng/mL IFNγ or with 10ng/mL IL-4/IL-13, respectively[132]. Cells were then stimulated with 100ng/mL LPS in the last 3hrs[132]. Collectively, these findings provide evidence that perhaps the culture methods used here were not appropriate to the objectives set out by this study. Further optimization would benefit from incorporating the above strategies.

Although the silent agonist of m-bromo PEP did not appear to modulate the expression of M1/M2 surface markers in human PBMCs, several lines of evidence indicate that cholinergic agonists acting through α7 nAChRs can modulate macrophage phenotype[55,102,133]. For instance, a study by Simard *et al.,* showed that in the bone marrow of LPS-challenged mice, the α7 agonist nicotine was able to reduce levels of inflammatory monocytes, subsequently diminishing the existing ratio between M1 and M2 monocytes[71]. In extension, a follow up study in 2019 by Simard *et al.,* showed that in mice, the silent agonist m-bromo PEP was able to significantly reduce the number of bone marrow-derived monocyte/macrophage numbers and inflammatory phenotype[91].

Thus, it is likely that the lack of effect on behalf of the silent agonist used in this study was due to the absence of an LPS effect. Another explanation was noted earlier in this project's investigation into silent agonist modulation of cytokine secretion. Indeed,

certain silent agonists appeared to function more effectively in humans versus mice. In particular, the silent agonist PCF_3 diEPP appeared to be highly effective with human cells, thus, it is possible that the silent agonist m-bromo PEP is only effective at modulating murine M1/M2 phenotyping. Subsequent investigations into silent agonist modulation of M1/M2 cell phenotype in humans should incorporate PCF_3 diEPP alongside other silent agonists.

6.0 Conclusion

To the best of knowledge, this study reports for the first time that silent agonists can counteract LPS-induced responses by human blood immune cells. The silent agonist PCF_3 diEPP inhibited the release of pro-inflammatory cytokines in whole blood and downregulated NFκB pathway activity by peripheral blood immune cells. While present findings could not indicate a role for silent agonist modulation of M1/M2 phenotype, further optimization will allow for appropriate evaluation. This study supports previous studies showing an anti-inflammatory role of α7 nAChRs through channel desensitization and contributes to the mechanistic understanding of nAChRs. Our findings implicate silent agonists as a therapeutic alternative for the treatment of autoimmune and inflammatory diseases.

Despite these findings, much work is still needed. Once experiments have been further optimized, future studies should investigate how silent agonists modulate intracellular signaling events in additional immune cells such as T and B cells, as they are implicated in the pathology of numerous diseases[19,31,58]. Furthermore, it has been shown that in the blood of MS patients, there are higher levels of pro-inflammatory cytokines

relative to patients without MS[134]. Thus, future experiments could shift to using blood ethically obtained from MS patients to further assess the potential of silent agonists to counteract inflammatory activity. Novel investigations involving α7-selective silent agonists will hopefully set the stage for phase 1 clinical studies and contribute to a lacking catalog of clinically sound α7-selective agonists.

7.0 References

1. Smith, D. A. & Germolec, D. R. Introduction to immunology and autoimmunity. *Environ. Health Perspect.* **107**, 661–665 (1999).

2. Marshall, J. S., Warrington, R., Watson, W. & Kim, H. L. An introduction to immunology and immunopathology. *Allergy, Asthma Clin. Immunol.* **14**, 1–8 (2018).

3. Chaplin, D. D. Overview of immune response. *J Allergy Clin Immunol.* **125**, 41 (2010).

4. Chen, L., Deng, H., Cui, H., Fang, J., Zuo, Z., Deng, J., Li, Y., Wang, X. & Zhao, L. Inflammatory responses and inflammation-associated diseases in organs. *Oncotarget* **9**, 7204–7218 (2018).

5. Teh, Y. C., Ding, J. L., Ng, L. G. & Chong, S. Z. Capturing the Fantastic Voyage of Monocytes Through Time and Space . *Frontiers in Immunology* vol. 10 834 (2019).

6. Parihar, A., Eubank, T. D. & Doseff, A. I. Monocytes and macrophages regulate immunity through dynamic networks of survival and cell death. *J. Innate Immun.* **2**, 204–215 (2010).

7. Naito, M., Yamamura, F., Nishikawa, S. & Takahashi, K. Development, Differentiation, and Maturation of Fetal Mouse Yolk Sac Macrophages in Cultures. *J. Leukoc. Biol.* **46**, 1–10 (1989).

8. Hoeffel, G. & Ginhoux, F. Fetal monocytes and the origins of tissue-resident macrophages. *Cell. Immunol.* **330**, 5–15 (2018).

9. Palis, J., Chan, R. J., Koniski, A., Patel, R., Starr, M. & Yoder, M. C. Spatial and temporal emergence of high proliferative potential hematopoietic precursors during murine embryogenesis. *Proc. Natl. Acad. Sci.* **98**, 4528 LP – 4533 (2001).

10. Travers, P., Walport, M. & Janeway, C. *Immunobiology: The Immune System in Health and Disease*. (Garland Science, 2001).

11. Weber, C., Belge, K.-U., von Hundelshausen, P., Draude, G., Steppich, B., Mack, M., Frankenberger, M., Weber, K. S. C. & Ziegler-Heitbrock, H. W. L. Differential chemokine receptor expression and function in human monocyte subpopulations. *J. Leukoc. Biol.* **67**, 699–704 (2000).

12. Geissmann, F., Jung, S. & Littman, D. R. Blood Monocytes Consist of Two Principal Subsets with Distinct Migratory Properties. *Immunity* **19**, 71–82 (2003).

13. Zawada, A. M., Rogacev, K. S., Rotter, B., Winter, P., Marell, R.-R., Fliser, D. & Heine, G. H. SuperSAGE evidence for CD14++CD16+ monocytes as a third monocyte subset. *Blood* **118**, e50-61 (2011).

14. Kumar, B. V., Connors, T. J. & Farber, D. L. Human T Cell Development, Localization, and Function throughout Life. *Immunity* **48**, 202–213 (2018).

15. Pennock, N. D., White, J. T., Cross, E. W., Cheney, E. E., Tamburini, B. A. & Kedl, R. M. T cell responses: naive to memory and everything in between. *Adv. Physiol. Educ.* **37**, 273–283 (2013).

16. Takeuchi, A. & Saito, T. CD4 CTL, a cytotoxic subset of CD4+ T cells, their differentiation and function. *Front. Immunol.* **8**, 1–7 (2017).

17. Abbas, A., Lichtman, A. & Pillai, S. *Cellular & Molecular Immunology*. (Elsevier B.V., 2018).

18. Romagnani, S. T-cell subsets (Th1 versus Th2). *Ann. Allergy, Asthma Immunol.* **85**, 9–21 (2000).

19. Raphael, I., Nalawade, S., Eagar, T. & Forsthuber, T. T cell subsets and their signature cytokines in autoimmune and inflammatory diseases. *Physiol. Behav.* **74**, 5–17 (2015).

20. Bhattacharya, M. Understanding B Lymphocyte Development: A Long Way to Go. *Intechopen* 41–51 (2018) doi:10.5772/intechopen.79663.

21. Hoffman, W., Lakkis, F. G. & Chalasani, G. B cells, antibodies, and more. *Clin. J. Am. Soc. Nephrol.* **11**, 137–154 (2016).

22. Matsushita, T., Yanaba, K., Bouaziz, J.-D., Fujimoto, M. & Tedder, T. F. Regulatory B cells inhibit EAE initiation in mice while other B cells promote disease progression. *J. Clin. Invest.* **118**, 3420–3430 (2008).

23. Cobb, M. H. MAP Kinase pathways. *Prog. Biophys. Mol. Biol.* **71**, 479–500 (1999).

24. Liu, T., Zhang, L., Joo, D. & Sun, S. C. NF-κB signaling in inflammation. *Signal Transduct. Target. Ther.* **2**, (2017).

25. Shi, H. & Berger, E. A. Characterization of site-specific phosphorylation of NF-κB p65 in retinal cells in response to high glucose and cytokine polarization. *Mediators Inflamm.* **2018**, (2018).

26. Harrison, D. The JAK / STAT Pathway : Fact Sheet. 1–3 (1990).

27. O'Shea, J., Schwartz, D., Villarino, A., Gadina, M., McInnes, L. & Laurence, A. The JAK-STAT Pathway: Impact on Human Disease and Therapeutic Intervention. *Physiol. Behav.* **176**, 139–148 (2015).

28. Shi, X., Wang, J., Lei, Y., Cong, C., Tan, D. & Zhou, X. Research progress on the PI3K/AKT signaling pathway in gynecological cancer (Review). *Mol. Med. Rep.* **19**, 4529–4535 (2019).

29. Vergadi, E., Ieronymaki, E., Lyroni, K., Vaporidi, K. & Tsatsanis, C. Akt Signaling Pathway in Macrophage Activation and M1/M2 Polarization. *J. Immunol.* **198**, 1006–1014 (2017).

30. Hemmings, B. A. & Restuccia, D. F. PI3K-PKB / Akt Pathway. 1–4 (2016).

31. Göbel, K., Ruck, T. & Meuth, S. G. Cytokine signaling in multiple sclerosis: Lost in translation. *Mult. Scler. J.* **24**, 432–439 (2018).

32. Turner, M. D., Nedjai, B., Hurst, T. & Pennington, D. J. Cytokines and chemokines: At the crossroads of cell signalling and inflammatory disease. *Biochim. Biophys. Acta - Mol. Cell Res.* **1843**, 2563–2582 (2014).

33. Iyer, S. S. & Cheng, G. Role of interleukin 10 transcriptional regulation in inflammation and autoimmune disease. *Crit. Rev. Immunol.* **32**, 23–63 (2012).

34. Fischer, R., Sendetski, M., del Rivero, T., Martinez, G. F., Bracchi-Ricard, V., Swanson, K. A., Pruzinsky, E. K., Delguercio, N., Rosalino, M. J., Padutsch, T., Kontermann, R. E., Pfizenmaier, K. & Bethea, J. R. TNFR2 promotes Treg-mediated recovery from neuropathic pain across sexes. *Proc. Natl. Acad. Sci. U. S. A.* **116**, 17045–17050 (2019).

35. Faustman, D. & Davis, M. TNF Receptor 2 and Disease: Autoimmunity and Regenerative Medicine . *Frontiers in Immunology* vol. 4 478 (2013).

36. Pobezinskaya, Y. L., Kim, Y.-S., Choksi, S., Morgan, M. J., Li, T., Liu, C. & Liu, Z. The function of TRADD in signaling through tumor necrosis factor receptor 1 and TRIF-dependent Toll-like receptors. *Nat. Immunol.* **9**, 1047–1054 (2008).

37. Micheau, O. & Tschopp, J. Induction of TNF Receptor I-Mediated Apoptosis via Two Sequential Signaling Complexes. *Cell* **114**, 181–190 (2003).

38. Smith, K. A. & Maizels, R. M. IL-6 controls susceptibility to helminth infection by impeding Th2 responsiveness and altering the Treg phenotype in vivo. *Eur. J. Immunol.* **44**, 150–161 (2014).

39. Takeda, K., Kaisho, T., Yoshida, N., Takeda, J., Kishimoto, T. & Akira, S. Correction: Stat3 Activation Is Responsible for IL-6–Dependent T Cell Proliferation through Preventing Apoptosis: Generation and Characterization of T Cell–Specific Stat3-Deficient Mice. *J. Immunol.* **194**, 3526–3526 (2015).

40. Suvas, S., Azkur, A. K., Kim, B. S., Kumaraguru, U. & Rouse, B. T. CD4+CD25+ regulatory T cells control the severity of viral immunoinflammatory lesions. *J. Immunol.* **172**, 4123–4132 (2004).

41. Rosenblum, M. D., Remedios, K. A. & Abbas, A. K. Mechanisms of human autoimmunity. *J. Clin. Invest.* **125**, 2228–2233 (2015).

42. Podbielska, M., Banik, N. L., Kurowska, E. & Hogan, E. L. Myelin recovery in multiple sclerosis: The challenge of remyelination. *Brain Sci.* **3**, 1282–1324 (2013).

43. Cai, J., Qi, Y., Hu, X., Tan, M., Liu, Z., Zhang, J., Li, Q., Sander, M. & Qiu, M. Generation of oligodendrocyte precursor cells from mouse dorsal spinal cord independent of Nkx6 regulation and Shh signaling. *Neuron* **45**, 41–53 (2005).

44. Ghasemi, N., Razavi, S. & Nikzad, E. Multiple sclerosis: Pathogenesis, symptoms, diagnoses and cell-based therapy. *Cell J.* **19**, 1–10 (2017).

45. Blonda, M., Amoruso, A., Grasso, R., Di Francescantonio, V. & Avolio, C. Multiple sclerosis treatments affect monocyte-derived microvesicle production. *Front. Neurol.* **8**, (2017).

46. Sharief, M. K. & Hentges, R. Association between Tumor Necrosis Factor-α and Disease Progression in Patients with Multiple Sclerosis. *N. Engl. J. Med.* **325**, 467–472 (1991).

47. Maimone, D., Guazzi, G. C. & Annunziata, P. IL-6 detection in multiple sclerosis brain. *J. Neurol. Sci.* **146**, 59–65 (1997).

48. Bettelli, E., Prabhu Das, M., Howard, E. D., Weiner, H. L., Sobel, R. A. & Kuchroo, V. K. IL-10 Is Critical in the Regulation of Autoimmune Encephalomyelitis as Demonstrated by Studies of IL-10- and IL-4-Deficient and Transgenic Mice. *J. Immunol.* **161**, 3299 LP – 3306 (1998).

49. Multiple Sclerosis Treatments. *Mayo Clinic* https://www.mayoclinic.org/diseases-

conditions/multiple-sclerosis/diagnosis-treatment/drc-20350274 (2019).

50. Huang, W. J., Chen, W. W. & Zhang, X. Multiple sclerosis: Pathology, diagnosis and treatments (review). *Exp. Ther. Med.* **13**, 3163–3166 (2017).

51. Mishra, M. K. & Wee Yong, V. Myeloid cells-targets of medication in multiple sclerosis. *Nat. Rev. Neurol.* **12**, 539–551 (2016).

52. Herz, J., Filiano, A. J., Smith, A., Yogev, N. & Kipnis, J. Myeloid Cells in the Central Nervous System. *Immunity* **46**, 943–956 (2017).

53. Martinez, F. O. & Gordon, S. The M1 and M2 paradigm of macrophage activation: Time for reassessment. *F1000Prime Rep.* **6**, 1–13 (2014).

54. Durafourt, B. A., Moore, C. S., Zammit, D. A., Johnson, T. A., Zaguia, F., Guiot, M. C., Bar-Or, A. & Antel, J. P. Comparison of polarization properties of human adult microglia and blood-derived macrophages. *Glia* **60**, 717–727 (2012).

55. Mikita, J., Dubourdieu-Cassagno, N., Deloire, M. S., Vekris, A., Biran, M., Raffard, G., Brochet, B., Canron, M. H., Franconi, J. M., Boiziau, C. & Petry, K. G. Altered M1/M2 activation patterns of monocytes in severe relapsing experimental rat model of multiple sclerosis. Amelioration of clinical status by M2 activated monocyte administration. *Mult. Scler. J.* **17**, 2–15 (2011).

56. House, D., Chinh, N. T., Hien, T. T., Parry, C. P., Ly, N. T., Diep, T. S., Wain, J., Dunstan, S., White, N. J., Dougan, G. & Farrar, J. J. Cytokine Release by Lipopolysaccharide-Stimulated Whole Blood from Patients with Typhoid Fever. *J. Infect. Dis.* **186**, 240–245 (2002).

57. Moehle, M. S. & West, A. B. M1 and M2 Immune Activation in PD. 59–73 (2016) doi:10.1016/j.neuroscience.2014.11.018.M1.

58. Li, R., Patterson, K. R. & Bar-Or, A. Reassessing B cell contributions in multiple sclerosis. *Nat. Immunol.* **19**, 696–707 (2018).

59. Albuquerque, E., Pereira, E., Alkondon, M. & Rogers, S. Mammalian Nicotinic Acetylcholine Receptors: From Structure to Function. *Physiol. Rev.* **89**, 73–120 (2009).

60. Kabbani, N. & Nichols, R. A. Beyond the Channel: Metabotropic Signaling by Nicotinic Receptors. *Trends Pharmacol. Sci.* **39**, 354–366 (2018).

61. H. Ferreira-Vieira, T., M. Guimaraes, I., R. Silva, F. & M. Ribeiro, F. Alzheimer's disease: Targeting the Cholinergic System. *Curr. Neuropharmacol.* **14**, 101–115 (2016).

62. Wonnacott, S. & Barik, J. Tocris Bioscience Scientific Review Series Nicotinic ACh Receptors. (2001).

63. Changeux, J. P. & Paas, Y. Nicotinic Acetylcholine Receptors. *Encycl. Neurosci.* 1129–1133 (2009) doi:10.1016/B978-008045046-9.01127-X.

64. Báez-Pagán, C. A., Delgado-Vélez, M. & Lasalde-Dominicci, J. A. Activation of the Macrophage α7 Nicotinic Acetylcholine Receptor and Control of Inflammation. *J. Neuroimmune Pharmacol.* **10**, 468–476 (2015).

65. Posadas, I., López-Hernández, B. & Ceña, V. Nicotinic Receptors in Neurodegeneration. *Curr. Neuropharmacol.* **11**, 298–314 (2013).

66. Bouzat, C., Lasala, M., Nielsen, B. E., Corradi, J. & Esandi, M. del C. Molecular function of α7 nicotinic receptors as drug targets. *J. Physiol.* **596**, 1847–1861 (2018).

67. Hao, J., Simard, A. R., Turner, G. H., Wu, J., Whiteaker, P., Lukas, R. J. & Shi, F. D. Attenuation of CNS inflammatory responses by nicotine involves α7 and non-α7 nicotinic receptors. *Exp. Neurol.* **227**, 110–119 (2011).

68. Shi, F.-D., Piao, W.-H., Kuo, Y.-P., Campagnolo, D. I., Vollmer, T. L. & Lukas, R. J. Nicotinic Attenuation of Central Nervous System Inflammation and Autoimmunity. *J. Immunol.* **182**, 1730–1739 (2009).

69. Gao, Z., Nissen, J. C., Ji, K. & Tsirka, S. E. The experimental autoimmune encephalomyelitis disease course is modulated by nicotine and other cigarette smoke components. *PLoS One* **9**, (2014).

70. Borovikova, L. V., Ivanova, S., Zhang, M., Yang, H., Botchkina, G. I., Watkins, L. R., Wang, H., Abumrad, N., Eaton, J. W. & Tracey, K. J. Vagus nerve stimulation attenuates the systemic inflammatory response to endotoxin. *Nature* **405**, 458–462 (2000).

71. St-Pierre, S., Jiang, W., Roy, P., Champigny, C., LeBlanc, É., Morley, B. J., Hao, J. & Simard, A. R. Nicotinic acetylcholine receptors modulate bone marrow-derived pro-inflammatory monocyte production and survival. *PLoS One* **11**, 1–18 (2016).

72. Thomsen, M. S. & Mikkelsen, J. D. The α7 nicotinic acetylcholine receptor ligands methyllycaconitine, NS6740 and GTS-21 reduce lipopolysaccharide-induced TNF-α release from microglia. *J. Neuroimmunol.* **251**, 65–72 (2012).

73. Horenstein, N. A. & Papke, R. L. Anti-inflammatory Silent Agonists. *ACS Med. Chem. Lett.* **8**, 989–991 (2017).

74. Corradi, J. & Bouzat, C. Understanding the Bases of Function and Modulation of 7 Nicotinic Receptors: Implications for Drug Discovery. *Mol. Pharmacol.* **90**, 288–299 (2016).

75. Wonnacott S. Nicotinic ACh receptors. *Tocris Biosci. Sci. Rev. Ser.* **Nicotinic**, 1–31 (2014).

76. Ochoa, E. L. M., Chattopadhyay, A. & McNamee, M. G. *Desensitization of the nicotinic acetylcholine receptor: Molecular mechanisms and effect of modulators*. *Cellular and Molecular Neurobiology* vol. 9 (1989).

77. Papke, R. L. The analgesic-like properties of the alpha7 nAChR silent agonist NS6740 is associated with non-conducting conformations of the receptor. **71**, 233–236 (2013).

78. Wonnacott, S., Bermudez, I., Millar, N. S. & Tzartos, S. J. Nicotinic acetylcholine receptors. *Br. J. Pharmacol.* **175**, 1785–1788 (2018).

79. Zdanowski, R., Krzyzowska, M., Ujazdowska, D., Lewicka, A. & Lewicki, S. Role of α7 nicotinic receptor in the immune system and intracellular signaling pathways. *Cent. Eur. J. Immunol.* **40**, 373–379 (2015).

80. De Jonge, W. J. & Ulloa, L. The alpha7 nicotinic acetylcholine receptor as a pharmacological target for inflammation. *Br. J. Pharmacol.* **151**, 915–929 (2007).

81. Cuoco, J. A. & Fennie, C. N. The Cholinergic Anti-Inflammatory Pathway: A Novel Paradigm for Translational Research in Neuroimmunology. *J. Neurol. Neurosci.* **7**, 1–7 (2016).

82. Joe, Y., Kim, H. J., Kim, S., Chung, J., Ko, M. S., Lee, W. H., Chang, K. C., Park, J. W. & Chung, H. T. Tristetraprolin mediates anti-inflammatory effects of nicotine in lipopolysaccharide-stimulated macrophages. *J. Biol. Chem.* **286**, 24735–24742 (2011).

83. Peña, G., Cai, B., Liu, J., van der Zanden, E. P., Deitch, E. A., de Jonge, W. J. & Ulloa, L. Unphosphorylated STAT3 modulates alpha 7 nicotinic receptor signaling and cytokine production in sepsis. *Eur. J. Immunol.* **40**, 2580–2589 (2010).

84. Giebelen, I. A. J., van Westerloo, D. J., LaRosa, G. J., de Vos, A. F. & van der Poll, T. Stimulation of alpha 7 cholinergic receptors inhibits lipopolysaccharide-induced neutrophil recruitment by a tumor necrosis factor alpha-independent mechanism. *Shock* **27**, 443–447 (2007).

85. Gubbins, E. J., Gopalakrishnan, M. & Li, J. α7 nAChR-mediated activation of MAP kinase pathways in PC12 cells. *Brain Res.* **1328**, 1–11 (2010).

86. Schaal, C. & Chellappan, S. P. Nicotine-mediated cell proliferation and tumor progression in smoking-related cancers. *Mol. Cancer Res.* **12**, 14–23 (2014).

87. Yue, Y., Liu, R., Cheng, W., Hu, Y., Li, J., Pan, X., Peng, J. & Zhang, P. GTS-21

attenuates lipopolysaccharide-induced inflammatory cytokine production in vitro by modulating the Akt and NF-κB signaling pathway through the α7 nicotinic acetylcholine receptor. *Int. Immunopharmacol.* **29**, 504–512 (2015).

88. Papke, R. L., Stokes, C., Damaj, M. I., Thakur, G. A., Manther, K., Treinin, M., Bagdas, D., Kulkarni, A. R. & Horenstein, N. A. Persistent activation of α7 nicotinic ACh receptors associated with stable induction of different desensitized states. *Br. J. Pharmacol.* **175**, 1838–1854 (2018).

89. Quadri, M., Bagdas, D., Toma, W., Stokes, C., Horenstein, N. A., Damaj, M. I. & Papke, R. L. The antinociceptive and anti-inflammatory properties of the a7 nAChR weak partial agonist p-CF3 N,N-diethyl-N9-phenylpiperazine. *J. Pharmacol. Exp. Ther.* **367**, 203–214 (2018).

90. Papke, R. L. Merging old and new perspectives on nicotinic acetylcholine receptors. *Biochem. Pharmacol.* **89**, 1–11 (2014).

91. Godin, J. R., Roy, P., Quadri, M., Bagdas, D., Toma, W., Narendrula-Kotha, R., Kishta, O. A., Damaj, M. I., Horenstein, N. A., Papke, R. L. & Simard, A. R. A silent agonist of α7 nicotinic acetylcholine receptors modulates inflammation ex vivo and attenuates EAE. *Brain. Behav. Immun.* 1–15 (2020) doi:10.1016/j.bbi.2019.12.014.

92. Quadri, M., Papke, R. L. & Horenstein, N. A. Dissection of N,N-diethyl-N′-phenylpiperazines as α7 nicotinic receptor silent agonists. *Bioorg. Med. Chem.* **24**, 286–293 (2016).

93. Villiger, Y., Szanto, I., Jaconi, S., Blanchet, C., Buisson, B., Krause, K. H., Bertrand, D. & Romand, J. A. Expression of an α7 duplicate nicotinic acetylcholine receptor-related protein in human leukocytes. *J. Neuroimmunol.* **126**, 86–98 (2002).

94. Skok, M. V. Editorial: To channel or not to channel? Functioning of nicotinic acetylcholine receptors in leukocytes. *J. Leukoc. Biol.* **86**, 1–3 (2009).

95. Gourlay, S. G. & Benowitz, N. L. Arteriovenous differences in plasma concentration of nicotine and catecholamines and related cardiovascular effects after smoking, nicotine nasal spray, and intravenous nicotine. *Clin. Pharmacol. Ther.* **62**, 453–463 (1997).

96. Blunt, C. E. W. & Dougherty, D. A. Binding Interactions of NS6740, a Silent Agonist of the α 7 Nicotinic Acetylcholine Receptor . *Mol. Pharmacol.* **96**, 212–218 (2019).

97. Duque, G. A. & Descoteaux, A. Macrophage cytokines: Involvement in immunity and infectious diseases. *Front. Immunol.* **5**, 1–12 (2014).

98. Hamano, R., Takahashi, H. K., Iwagaki, H., Yoshino, T., Nishibori, M. & Tanaka, N. Stimulation of α7 nicotinic acetylcholine receptor inhibits CD14 and the toll-like receptor 4 expression in human monocytes. *Shock* **26**, 358–364 (2006).

99. Garg, B. K. & Loring, R. H. GTS-21 has cell-specific anti-inflammatory effects independent of α7 nicotinic acetylcholine receptors. *PLoS One* **14**, 1–16 (2019).

100. Liu, Q., Liu, C., Jiang, L., Li, M., Long, T., He, W., Qin, G., Chen, L. & Zhou, J. α7 nicotinic acetylcholine receptor-mediated anti-inflammatory effect in a chronic migraine rat model via the attenuation of Glial cell activation. *J. Pain Res.* **11**, 1129–1140 (2018).

101. Wilking, J. & Stitzel, J. Natural Genetic Variability of the Neuronal Nicotinic Acetylcholine Receptor Subunit Genes in Mice: Consequences and Confounds. *Neuropharmacology* **96**, 205–212 (2015).

102. de Jonge, W. J., van der Zanden, E. P., The, F. O., Bijlsma, M. F., van Westerloo, D. J., Bennink, R. J., Berthoud, H. R., Uematsu, S., Akira, S., van den Wijngaard, R. M. & Boeckxstaens, G. E. Stimulation of the vagus nerve attenuates macrophage activation by activating the Jak2-STAT3 signaling pathway. *Nat. Immunol.* **6**, 844–851 (2005).

103. Ibrahim, S. M., Al-Shorbagy, M. Y., Abdallah, D. M. & El-Abhar, H. S.

Activation of α7 Nicotinic Acetylcholine Receptor Ameliorates Zymosan-Induced Acute Kidney Injury in BALB/c Mice. *Sci. Rep.* **8**, 2–11 (2018).

104. Liu, Y., Wu, D., Song, F., Zhu, C., Hui, Y., Zhu, Q., Wu, J., Fan, W. & Hu, J. Activation of α7 nicotinic acetylcholine receptors prevents monosodium iodoacetate-induced osteoarthritis in rats. *Cell. Physiol. Biochem.* **35**, 627–638 (2015).

105. Yoshikawa, H., Kurokawa, M., Ozaki, N., Nara, K., Atou, K., Takada, E., Kamochi, H. & Suzuki, N. Nicotine inhibits the production of proinflammatory mediators in human monocytes by suppression of I-κB phosphorylation and nuclear factor-κB transcriptional activity through nicotinic acetylcholine receptor α7. *Clin. Exp. Immunol.* **146**, 116–123 (2006).

106. Mussbacher, M., Salzmann, M., Brostjan, C., Hoesel, B., Schoergenhofer, C., Datler, H., Hohensinner, P., Basílio, J., Petzelbauer, P., Assinger, A. & Schmid, J. A. Cell type specific roles of nf-kb linking inflamation and thrombosis. *Front. Immunol.* **10**, 1–31 (2019).

107. Fong, C. H. Y., Bebien, M., Didierlaurent, A., Nebauer, R., Hussell, T., Broide, D., Karin, M. & Lawrence, T. An antiinflammatory role for IKKβ through the inhibition of 'classical' macrophage activation. *J. Exp. Med.* **205**, 1269–1276 (2008).

108. Ye, X., Jiang, X., Guo, W., Clark, K. & Gao, Z. Overexpression of NFkB p65 in Macrophages ameliorates atherosclerosis in apoE-knockout mice. *Am. J. Physiol.* **305**, 1375–1383 (2013).

109. Pradère, J. P., Hernandez, C., Koppe, C., Friedman, R. A., Luedde, T. & Schwabe, R. F. Negative regulation of NF-κB p65 activity by serine 536 phosphorylation. *Sci. Signal.* **9**, (2016).

110. Seyedabadi, M., Rahimian, R. & Ghia, J. E. The role of alpha7 nicotinic acetylcholine receptors in inflammatory bowel disease: involvement of different

cellular pathways. *Expert Opin. Ther. Targets* **22**, 161–176 (2018).

111. Aicher, A., Heeschen, C., Mohaupt, M., Cooke, J. P., Zeiher, A. M. & Dimmeler, S. Nicotine strongly activates dendritic cell-mediated adaptive immunity: Potential role for progression of atherosclerotic lesions. *Circulation* **107**, 604–611 (2003).

112. Przanowski, P., Dabrowski, M., Ellert-Miklaszewska, A., Kloss, M., Mieczkowski, J., Kaza, B., Ronowicz, A., Hu, F., Piotrowski, A., Kettenmann, H., Komorowski, J. & Kaminska, B. The signal transducers Stat1 and Stat3 and their novel target Jmjd3 drive the expression of inflammatory genes in microglia. *J. Mol. Med.* **92**, 239–254 (2014).

113. Jiang, K., Chen, Y. & Jarvis, J. . Soluble Factors From LPS- and PHA-Activated PBMC Induce MAPK, STAT1, and STAT3 Phosphorylation in Primary Cultures of Human Term Placental Trophoblasts: Implications for Infection and Prematurity. *Placenta* **28**, 542 (2007).

114. Ganguly, G., Giang, P., Basu, S. & Mir, F. Mycobacterium tuberculosis 6-kDa Early Secreted Antigenic Target (ESAT-6) protein downregulates Lipopolysaccharide induced c-myc expression by modulating the Extracellular Signal Regulated Kinases 1/2. *BMC Immunol.* **8**, 24 (2007).

115. Guha, M. & Mackman, N. The Phosphatidylinositol 3-Kinase-Akt Pathway Limits Lipopolysaccharide Activation of Signaling Pathways and Expression of Inflammatory Mediators in Human Monocytic Cells. *J. Biol. Chem.* **277**, 32124–32132 (2002).

116. Ismail, H. A. H. A., Kang, B. H., Kim, J. S., Lee, J. H., Choi, I. W., Cha, G. H., Yuk, J. M. & Lee, Y. H. IL-12 and IL-23 production in Toxoplasma Gondii- or LPS-treated jurkat T cells via PI3K and MAPK signaling pathways. *Korean J. Parasitol.* **55**, 613–622 (2017).

117. Bagaev, A. V., Garaeva, A. Y., Lebedeva, E. S., Pichugin, A. V., Ataullakhanov, R. I. & Ataullakhanov, F. I. Elevated pre-activation basal level of nuclear NF-κB

in native macrophages accelerates LPS-induced translocation of cytosolic NF-κB into the cell nucleus. *Sci. Rep.* **9**, 1–16 (2019).

118. Khodarev, N. N., Roizman, B. & Weichselbaum, R. R. Molecular pathways: Interferon/Stat1 pathway: Role in the tumor resistance to genotoxic stress and aggressive growth. *Clin. Cancer Res.* **18**, 3015–3021 (2012).

119. Sikorski, K., Czerwoniec, A., Bujnicki, J. M., Wesoly, J. & Bluyssen, H. A. R. STAT1 as a novel therapeutical target in pro-atherogenic signal integration of IFNγ, TLR4 and IL-6 in vascular disease. *Cytokine Growth Factor Rev.* **22**, 211–219 (2011).

120. Greenhill, C. J., Rose-John, S., Lissilaa, R., Ferlin, W., Ernst, M., Hertzog, P. J., Mansell, A. & Jenkins, B. J. IL-6 Trans -Signaling Modulates TLR4-Dependent Inflammatory Responses via STAT3 . *J. Immunol.* **186**, 1199–1208 (2011).

121. Schmitz, K., Lang, H., Wohlschlaeger, J., Sotiropoulos, G., Reis, H., Schmid, K. & Baba, H. AKT and ERK1/2 signaling in intrahepatic cholangiocarcinoma. *World J. Gastroenterol.* **13**, 6470–6477 (2007).

122. Gentilini, D., Busacca, M., Di Francesco, S., Vignali, M., Vigano, P. & Di Blasio, A. . PI3K/Akt And ERK1/2 signalling pathways are involved in endometrial cell migration induced by 17β-estradiol and growth factors. *Mol. Hum. Reprod.* **13**, 317–322 (2007).

123. Yang, Y. H., Li, D. L., Bi, X. Y., Sun, L., Yu, X. J., Fang, H. Le, Miao, Y., Zhao, M., He, X., Liu, J. J. & Zang, W. J. Acetylcholine Inhibits LPS-Induced MMP-9 Production and Cell Migration via the 7 nAChR-JAK2/STAT3 Pathway in RAW264.7 Cells. *Cell. Physiol. Biochem.* **36**, 2025–2038 (2015).

124. Landmann, R., Ludwig, C., Obrist, R. & Obrecht, J. P. Effect of cytokines and lipopolysaccharide on CD14 antigen expression in human monocytes and macrophages. *J. Cell. Biochem.* **47**, 317–329 (1991).

125. Chou, M. H., Chuang, J. H., Eng, H. L., Tsai, P. C., Hsieh, C. S., Liu, H. C.,

Wang, C. H., Lin, C. Y. & Lin, T. M. Effects of hepatocyte CD14 upregulation during cholestasis on endotoxin sensitivity. *PLoS One* **7**, 1–11 (2012).

126. Hashimoto, R., Kakigi, R., Nakamura, K., Itoh, S., Daida, H., Okada, T. & Katoh, Y. LPS enhances expression of CD204 through the MAPK/ERK pathway in murine bone marrow macrophages. *Atherosclerosis* **266**, 167–175 (2017).

127. Serbina, N. V & Pamer, E. G. Monocyte emigration from bone marrow during bacterial infection requires signals mediated by chemokine receptor CCR2. *Nat. Immunol.* **7**, 311–317 (2006).

128. Cazareth, J., Guyon, A., Heurteaux, C., Chabry, J. & Petit-Paitel, A. Molecular and cellular neuroinflammatory status of mouse brain after systemic lipopolysaccharide challenge: importance of CCR2/CCL2 signaling. *J. Neuroinflammation* **11**, 132 (2014).

129. Singh-Jasuja, H., Thiolat, A., Ribon, M., Boissier, M. C., Bessis, N., Rammensee, H. G. & Decker, P. The mouse dendritic cell marker CD11c is down-regulated upon cell activation through Toll-like receptor triggering. *Immunobiology* **218**, 28–39 (2013).

130. Wang, H., Yan, F. L., Cunningham, M., Deng, Q. W., Zuo, L., Xing, F. L., Shi, L. H., Hu, S. S. & Huang, Y. Potential specific immunological indicators for stroke associated infection are partly modulated by sympathetic pathway activation. *Oncotarget* **7**, 52404–52415 (2016).

131. Mia, S., Warnecke, A., Zhang, X. M., Malmström, V. & Harris, R. A. An optimized protocol for human M2 macrophages using M-CSF and IL-4/IL-10/TGF-β yields a dominant immunosuppressive phenotype. *Scand. J. Immunol.* **79**, 305–314 (2014).

132. Awad, F., Assrawi, E., Jumeau, C., Georgin-Lavialle, S., Cobret, L., Duquesnoy, P., Piterboth, W., Thomas, L., Stankovic-Stojanovic, K., Louvrier, C., Giurgea, I., Grateau, G., Amselem, S. & Karabina, S. A. Impact of human monocyte and

macrophage polarization on NLR expression and NLRP3 inflammasome activation. *PLoS One* **12**, 1–18 (2017).

133. Zhang, Q., Lu, Y., Bian, H., Guo, L. & Zhu, H. Activation of the α7 nicotinic receptor promotes lipopolysaccharide-induced conversion of M1 microglia to M2. *Am. J. Transl. Res.* **9**, 971–985 (2017).

134. Kouwenhoven, M., Teleshova, N., Özenci, V., Press, R. & Link, H. Monocytes in multiple sclerosis: Phenotype and cytokine profile. *J. Neuroimmunol.* **112**, 197–205 (2001).